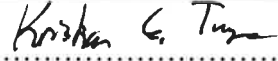# u$

Universitetet
i Stavanger

FACULTY OF SCIENCE AND TECHNOLOGY

MASTER'S THESIS

Study programme/specialisation: Engineering structures and Materials / Building structures	Spring semester, 2019 Open
Author: Kristian Goa Tunge	*Krishan G. Tunge* .... (signature of author)

Programme coordinator: Samindi Samarakoon

Supervisor(s): Samindi Samarakoon

Title of master's thesis:

Comparison of different design guidelines for steel fibre reinforced concrete (SFRC) structures

Credits: 30

Keywords: SFRC Fibre Reinforced Concrete Shear Crack-width Finite Element Method Nonlinear analysis	Number of pages: 65 +supplemental material/other: 16 Stavanger, 14.06.2019 date/year

COMPARISON OF DIFFERENT DESIGN GUIDELINES FOR STEEL FIBRE REINFORCED CONCRETE (SFRC) STRUCTURES

COMPARING THE SHEAR AND CRACK-WIDTH CALCULATIONS OF SFRC STRUCTURES
FROM EN 1992-1-1:2018, NB38,
AND FIB MODEL CODE 2010
WITH RESULTS FROM FEM

KRISTIAN TUNGE

University of Stavanger
Department of Mechanical and Structural Engineering and Materials Science
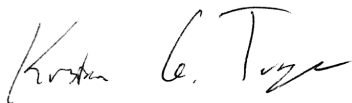
U S

2019
STAVANGER

Acknowledgement

Abstract

One of the main reasons for the limited use of steel fibre reinforced concrete (SFRC) in load-carrying structures today is the lack of accepted design guidelines. The Norwegian Concrete Association (Norsk Betongforening) are currently working on the publication NB38 - Guideline for design, execution, and control of fibre reinforced concrete in load-carrying structures, and a new version of EN 1992-1-1 is on it's way. Both of them include design guidelines for fibre reinforced concrete.

The primary aim of this thesis is to compare the new guidelines, along with existing guidelines, with respect to their calculations for shear resistance and crack-width. A theoretical study is carried out, comparing the theoretical shear resistance and crack-width for concrete classes defined in EN 1992-1-1:2018 Annex L.

For crack-widths, results from EN 1992-1-1:2018, NB38, and FIB Model Code 2010 are compared theoretically and for shear capacity, calculations from the different guidelines are compared to each other, as well as to results from finite element analyses.

The results show that the differences between the guidelines are vast, both for crack-widths and shear capacity. It is shown that some of the guidelines dramatically overestimate the contribution of fibres to the load-bearing capacity, while others underestimate it.

Sammendrag

Bruken av fiberarmert betong i bærende betongkonstruksjoner er i Norge minimal, det er hovedsaklig begrenset til bruk i gulv på grunn og som sprøytebetong. En av grunnene til dette er mangelen på aksepterte standarder for beregning og utførelse av fiberarmert betong. Norsk Betongforening jobber med en ny publikasjon per dags dato - NB38 - Veileder for prosjektering, utførelse og kontroll av fiberarmert betong i bærende konstruksjoner, og en ny versjon av betongstandarden EN 1992-1-1 er under arbeid. Begge med beregningsmetoder for stålfiberarmert betong.

Hovedmålet med oppgaven er å sammenligne beregningsmetodene fra EN 1992-1-1:2018, NB38, i tillegg til FIB Model Code 2010, når det gjelder skjærkapasitet og rissberegninger. En teoretisk studie er utført, med mål om å sammenligne de teoretiske skjærkapasitetene og rissviddene for flere av klassene definert i EN 1992-1-1:2018 Annex L.

For rissviddeberegninger sammenliknes resultatene fra de forskjellige standardene teoretisk. For skjærkapasitet vil resultatene fra de forskjellige standardene i tillegg til å sammenliknes mot hverandre, sammenliknes mot resultater fra numerisk analyse ved hjelp av elementmetoden.

Resultatene viser at det er store forskjeller mellom resultatene fra de forskjellige standardene, både når det kommer til rissvidder og skjærkapasitet. Det er oppsiktsvekkende at noen av standardene i enkelte tilfeller dramatisk overvurderer stålfibrenes bidrag til betongens skjærkapasitet.

VI

Contents

List of Figures

X

List of Tables

Notations

Latin Upper Case Letters

A	Cross sectional area
A_c	Cross sectional area of concrete
$A_{c,ef}$	Effective concrete area
A_{ct}	Involved tension zone in the concrete of the cracked cross-sections of an equilibrium system in m²
A_s	Cross sectional area of ordinary reinforcement
A_{sw}	Cross sectional area of shear reinforcement
$CMOD_1$	=0.5mm is the crack width for which the characteristic residual flexural strength, $f_{R,1k}$, is determined from the beam test
$CMOD_3$	=2.5mm is the crack width for which the characteristic residual flexural strength, $f_{R,3k}$, is determined from the beam test
D_{lower}	Smallest value of the sieve size of the coarsest fraction of aggregates permitted by the specification of concrete
E_s	Design value of modulus of elasticity of ordinary reinforcing steel
V_{Rd}	Design Value of shear resistance

Latin Lower Case Letters

b_w	The minimum width of the cross-section between tension and compression chords
c	Concrete cover of reinforcement (to the surface of the bar)
d	Effective depth of a cross-section
d_{dg}	Size parameter for describing the crack and the failure zone roughness taking account of concrete type and its aggregate properties
f_{cd}	Design value of concrete compressive strength
f_{ck}	Characteristic compressive cylinder strength of concrete in [MPa] at age t_{ref}
f_{cm}	Mean concrete cylinder compressive strength at age t_{ref}
f_{ctm}	Mean axial tensile strength of concrete at age t_{ref}
f_{Ftsk}	Characteristic residual tensile strength for crack widths within the serviceability limit states
f_{Ftsm}	Mean residual concrete strength for crack widths within the serviceability limit states
f_{Ftud}	Design value of the residual tensile strength accounting for fibre orientation and volume effects
f_{Ftuk}	Characteristic residual tensile strength
$f_{Ftu,ef}$	Effective residual tensile strength for a given crack width accounting for fibre orientation and volume effects
$f_{R,1k}$	Characteristic residual flexural strength at $CMOD_1$=0.5mm
$f_{R,1m}$	Mean residual flexural strength at $CMOD_1$=0.5mm
$f_{R,3k}$	Characteristic residual flexural strength at $CMOD_3$=2.5mm
$f_{R,3m}$	Mean Residual flexural strength at $CMOD_3$=2.5mm
$f_{ftk,res2,5}$	Characteristic residual tensile strength at $CMOD_3$=2.5mm
f_{yd}	The yield strength which has been used to design the flexural reinforcement
f_{ywd}	Design yield strength of shear reinforcement

h	Overall depth of a cross-section or of a part of a cross-section
k_b	Coefficient which takes account of the bond properties of the bonded reinforcement for calculating the anchorage length
s	Spacing of the shear reinforcement measured along the longitudinal axis of the member
$s_{r,max,cal}$	Calculated maximum crack spacing when cracking is stabilized or alternatively the maximum length along which there is slip between concrete and steel in the phase of crack formation
t_{ref}	Age of concrete at which the concrete strength is determined in days
z	Inner lever arm of internal forces, for a member with constant depth, corresponding to the bending moment in the element under consideration

Greek Letters

α_{t3}	Conversion factor from residual flexural to residual tensile strength for crack openings in the ultimate range of CMOD_3
γ_c	Partial factor of safety for concrete
γ_{sf}	Partial factor of safety for SFRC
ε_{sh}	Shrinkage strain
η_r	Coefficient for considering the shrinkage contribution in crack width calculations
κ_G	Factor taking into account the volume effects in a SFRC member
κ_O	Factor taking into account the orientation of the steel fibres in the concrete matrix in relation to the orientation of the principle longitudinal stress arising from the action effects
ρ	Reinforcement ratio
ρ_l	Reinforcement ratio for bonded longitudinal reinforcement in the tensile zone due to bending referred to the nominal concrete area $d \cdot b_w$
$\rho_{p,ef}$	Tensile reinforcement ratio accounting for the different bond properties of reinforcing bars and prestressing tendons, referred to the effective concrete area
$\rho_{s,ef}$	Ratio between reinforcement area and the effective area of concrete in tension
σ_s	The steel stress in a crack
σ_{sr}	The maximum steel stress in a crack formation stage
τ_{bm}	The mean bond strength between steel and concrete
$\tau_{Rd,c}$	Shear stress resistance of members without shear reinforcement (average shear over a cross-section)
$\tau_{Rdc,min}$	Minimum shear stress resistance allowing to avoid a detailed verification for shear (average shear stress over a cross-section)
ϕ	Diameter of a reinforcing bar

Abbreviations

CMOD	Crack Mouth Opening Displacement
FRC	Fibre Reinforced Concrete
SFRC	Steel Fibre Reinforced Concrete

1 Introduction

1.1 Background

The use of Fibre Reinforced Concrete (FRC) is not a new idea, but the structural use of it hasn't been significant until recent years, and the main use of it today is limited to slabs on ground and sprayed concrete. One of the reasons for this is the lack of relevant design guidelines regarding the use of fibres in concrete dimensioning.

The lack of design guidelines is now seeing an end, and several standards are starting to appear - and even more are in the final stages before publishing. This thesis will look at the following standards;

- Final Version of EN 1992-1-1:2018 per April 2019. Scheduled to be completed in 2020

- Latest Version of NB38 - The Norwegian Concrete Association Publication nr 38. Scheduled

- fib Model Code 2010 - Existing standard describing the use of fibre reinforced concrete

One of the reasons for the lack of standards is the difficulties in calculations because the fibre-concrete interaction is a complex phenomenon dependent on a number of parameters (fig. 1.1). The effect on shear resistance and crack development are two of the main problems.
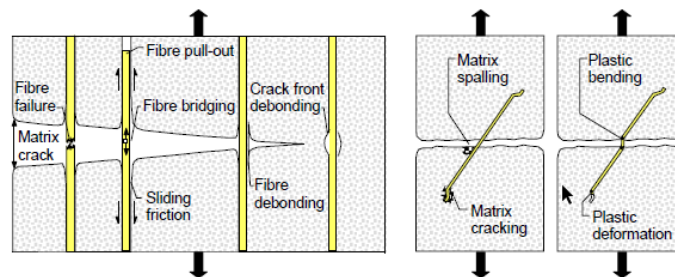
Figure 1.1: Mechanisms contributing to energy dissipation in cracks of FRC (Löfgren; 2005)

This thesis will look at how the different available guidelines calculate crack-widths and shear resistance, compare them, and compare the shear resistance given by the guidelines to shear resistances obtained by finite element analyses.

It is noted that all calculations based on NB38 and EN 1992-1-1:2018 are subject to change, and the formulas in the final versions of NB38 and EN 1992 may be different than the ones shown in this thesis.

2 Theoretical Background

2.1 General - FRC

Concrete containing cement, water, fine and coarse aggregates, and dispersed fibres is generally called Fibre Reinforced Concrete (FRC). The fibre content is generally less than 1% (Nordbrøden and Weydahl; 2012)

For fibres to be effective in cementitious matrices, it has been found that they should have the following properties (Naaman; 2003):

- A tensile strength significantly higher than the matrix (two to three orders of magnitude)

- A bond strength with the matrix of the same order as, or higher, than the tensile strength of the matrix

- An elastic modulus in tension significantly higher than that of the matrix (at least 3x)

- Enough ductility so that the fibre does not fracture due to fibre abrasion or bending

- The Poisson ratio and the coefficient of thermal expansion should preferably be of the same order

2.2 Types of Fibres

A wide range of fibre types (Figure 2.1) are commercially available in Norway, that are all used to improve toughness and other properties of concrete, e.g. reducing crack widths, reducing plastic shrinkage, or to avoid spalling of concrete during fire. Common materials are steel, carbon, glass, polyvinyl alcohol (PVA), polypropylene (PP), and cellulose (Døssland; 2008). Both the mechanical and geometrical properties of the fibres, and the effect they have on the concrete vary extensively. This thesis focuses on fibres used for structural applications, and for this purpose slender, high strength steel fibres are considered to be most efficient (Døssland; 2008; Kanstad et al.; 2011).
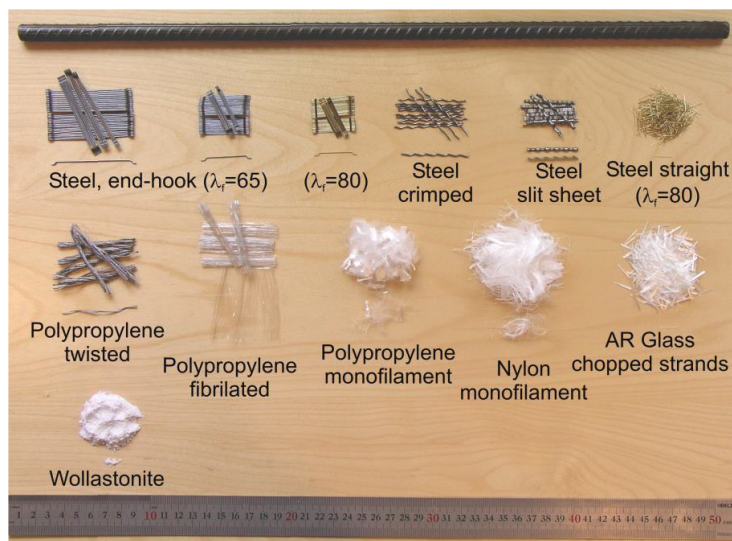
Figure 2.1: Types of commercially available fibres (Löfgren; 2005)

The geometry of the fibres has a large effect on the bond characteristics, and thus the fibres can be straight, coned, indented, crimped, end-hooked etc. to alter the performance (Figure 2.2)
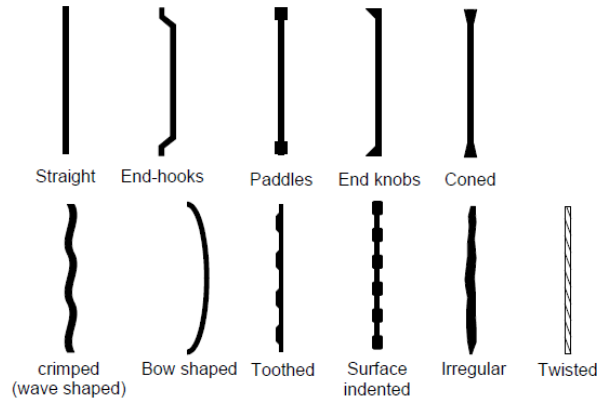
Figure 2.2: Examples of fibre geometries (Löfgren; 2005)

2.3   Fibre orientation and distribution

The orientation of the fibres in the mix plays an important role in the resulting mechanical performance of the fibre reinforced concrete (FRC), and the post-crack tensile strength depends strongly on the distribution and orientation of the fibres (Kanstad et al.; 2011). Fibres are most effective when they are located perpendicular to the crack, and when the crack appears at the middle of the fibre (Löfgren; 2005). For this, the efficiency factor η_0, also called the capacity factor, is defined. It's defined as the efficiency of bridging, i.e. how much of the fibre forces that are effective normal to the crack plane (Figure 2.3). The capacity factor is $\frac{1}{3}$ for isotropic orientation, $\frac{1}{2}$ when the fibres are plane oriented, and equal to 1 if all the fibres are directed normal to the crack plane (Døssland; 2008). Simplified, the efficiency factor η_0 can be taken as (*NB38*; n.d.):

$$\eta_0 = \tfrac{2}{3} \cdot \alpha \qquad \text{when} \qquad 0.3 < \alpha < 0.5$$

$$\eta_0 = \tfrac{4}{3} \cdot \alpha - \tfrac{1}{3} \quad \text{when} \qquad 0.5 < \alpha < 0.8$$

Where the orientation factor, α, is defined as $\alpha = \frac{\rho}{v_f} = \frac{n_f \cdot A_f}{v_f \cdot A_c}$, and where v_f is the fibre volume, n_f is the number of fibres, A_f is the area of a single fibre, and A_c is the cross sectional area of the section.
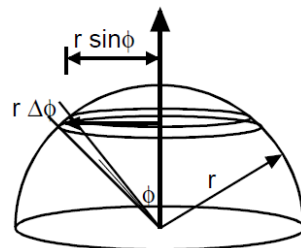
Figure 2.3: Determination of force resultant in the fibres crossing a crack. (Thorenfeldt; 2003)

Fibres tend to orientate parallel to the boundaries, thus, the orientation gets increasingly two-dimensional with decreasing thickness of the section (Figure 2.5 (c)). To account for this, the following equation for the orientation factor, α, may be used (Rosenbusch; 2003):

$\alpha = 0.382e^{-0.0033h} + 0.37$

Where h is the thickness of the cross section.
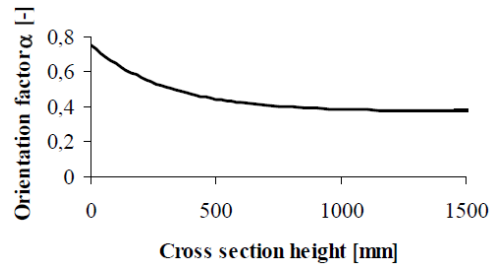
Figure 2.4: Effect of boundaries - Fibre orientation factor as a function of cross-section height. (Rosenbusch; 2003)
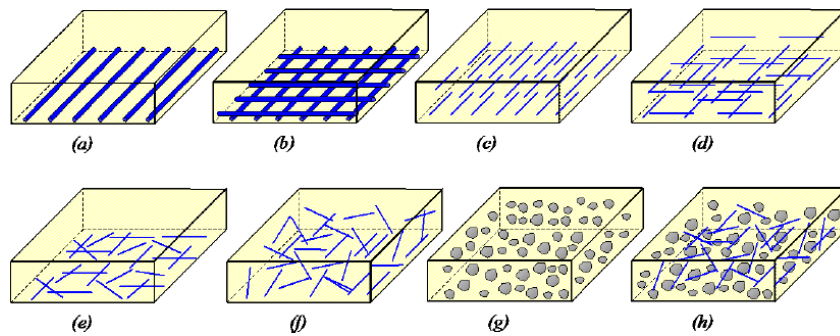
Figure 2.5: Schematic representation of different fibre composites: (a) unidirectional continuous; (b) bi-directional continuous; (c) discontinuous with biased 1-D fibre orientation; (d) discontinuous with biased 2-D fibre orientation; (e) discontinuous with plane-random orientation; (f) discontinuous with random fibre orientation; (g) particulate composite (particle suspension); and (h) fibre-reinforced and particulate composite (e.g. fibre-reinforced concrete). (Löfgren; 2005)

2.4 Shear behaviour of SFRC

In ordinary reinforced concrete, the principal action of transferring the shear stress across a crack is explained as friction at the crack faces aggregate interlock and dowel action (fig. 2.6). For ordinary reinforced concrete, the amount of reinforcement crossing the shear plane influences the shear capacity and shear friction due to dowel effects, and a similar effect can be seen in fibre reinforced concrete (Löfgren; 2005) (fig. 2.7). For fibre reinforced concrete with a low or moderate fibre dosage, the cracking strength is not improved, but once the matrix reaches it's tensile strength and starts to crack, the fibres are activated and starts to be pulled out (fig. 1.1) (Barragan; 2002).
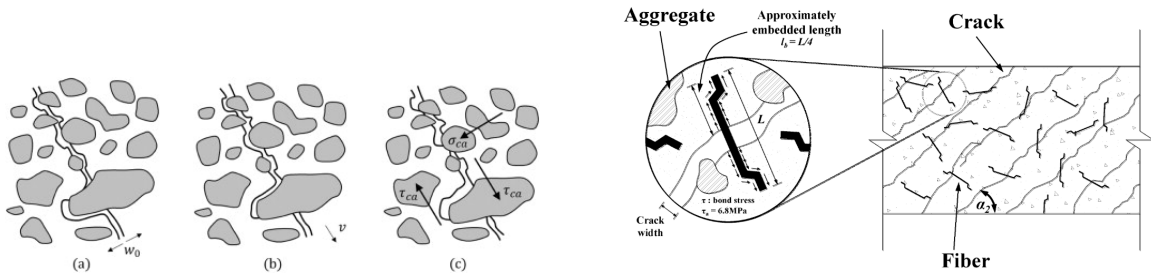
Figure 2.6: Aggregate interlock action: (a) initial crack opening due to tension; (b) longitudinal sliding reinstating contact between crack faces; (c) crack kinematics and generation of normal and shear stresses. (Micallef et al.; 2014)

Figure 2.7: Bond stress along steel fibre in a crack (Hwang et al.; 2013)

2.5 Crack development in SFRC

The matrix in concrete is very brittle, and is thus hard to prevent from cracking under tensile stresses. While uncracked, the matrix transfers a part of the stresses to the fibres. Once the matrix starts cracking, the fibres activate completely and transfers the stresses through the crack due to a number of mechanisms acting simultaneously (i.e. debonding, fibre pull-out, matrix spalling, and plastic deformations). Compared to ordinary rein-forced concrete, the fibres in SFRC act as an additional bridging mechanism, shown in fig. 2.8b (Löfgren; 2005).

(a)

(b)
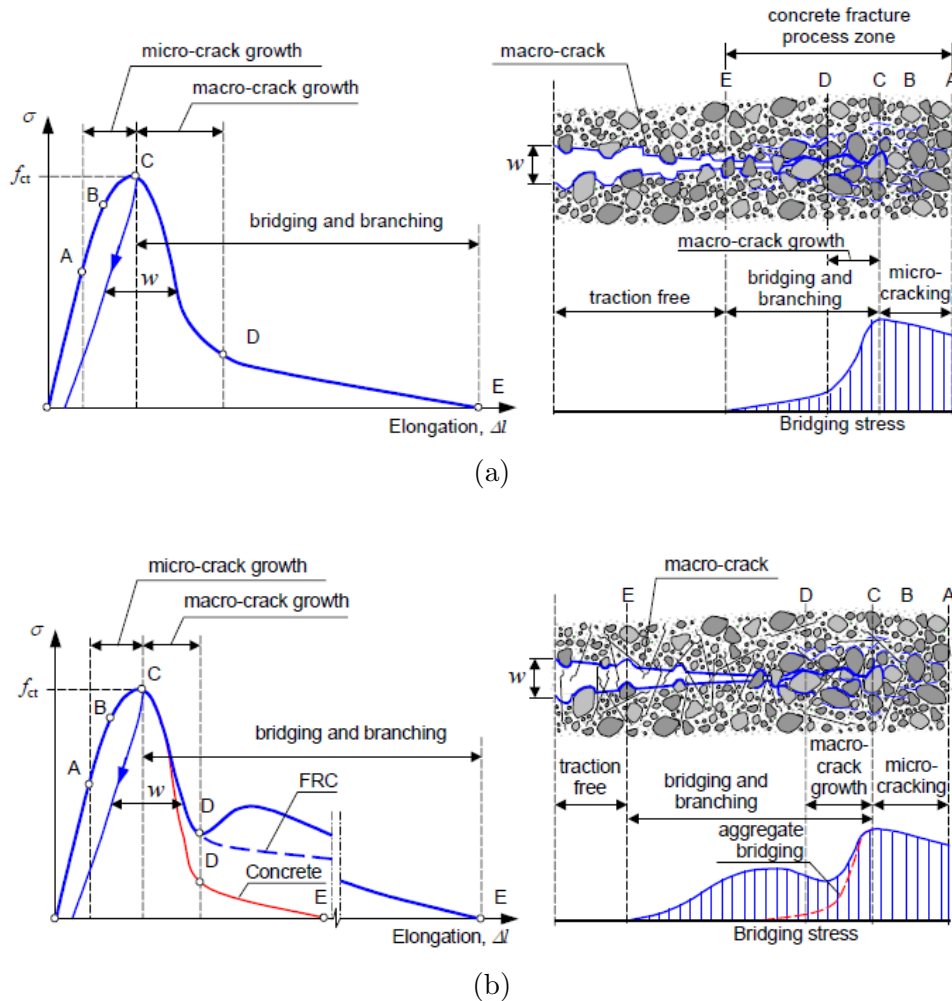
Figure 2.8: Schematic description of the fracture process in uni-axial tension of a) ordinary concrete and b) FRC (Löfgren; 2005)

2.6 Finite Element Method

The theories and formulas shown in sections 2.6.1 to 2.6.4 are based on the theories of the software used in this thesis, i.e. Atena by Červenka Consulting.

2.6.1 Material Model Formulation

The material model formulation is based on decomposing the strain ε_{ij} into elastic ε_{ij}^e, plastic ε_{ij}^p and fracturing ε_{ij}^f components (Borst; 1986).

$$\varepsilon_{ij} = \varepsilon_{ij}^e + \varepsilon_{ij}^p + \varepsilon_{ij}^f \tag{2.1}$$

The new stress state is then computed by equation 2.2

$$\sigma_{ij}^n = \sigma_{ij}^{n-1} + E_{ijkl}(\Delta\varepsilon_{kl} - \Delta\varepsilon_{kl}^p - \Delta\varepsilon_{kl}^f) \tag{2.2}$$

Where the increments of plastic strain $\Delta\varepsilon_{ij}^p$ and fracturing strain $\Delta\varepsilon_{ij}^f$ needs to be evaluated based on the material models used.

2.6.2 Plasticity Model for Concrete Crushing

The new stress state in the plastic model is computed using the predictor-corrector formula:

$$^{(n)}\sigma_{ij} = {}^{(n-1)}\sigma_{ij} + E_{ijkl}(\Delta\varepsilon_{kl} - \Delta\varepsilon_{kl}^p) = \sigma_{ij}^t - E_{ijkl}\Delta\varepsilon_{kl}^p = \sigma_{ij}^t - \sigma_{ij}^p \tag{2.3}$$

The plastic corrector factor σ_{ij}^p is calculated directly from the yield function:

$$F^p(\sigma_{ij}^t - \sigma_{ij}^p) = F^p(\sigma_{ij}^t - \Delta\lambda l_{ij}) = 0 \tag{2.4}$$

Where the return direction, l_{ij} can be defined as:

$$l_{ij} = E_{ijkl}\frac{\partial G^p(\sigma_{kl}^t)}{\partial\sigma_{kl}}, \text{ then } \Delta\varepsilon_{ij}^p = \Delta\lambda\frac{\partial G^p(\sigma_{ij}^t)}{\partial\sigma_{ij}} \tag{2.5}$$

Where $G(\sigma_{ij})$ is the plastic potential function.

In Atena, the failure surface of William Menetrey is used (Červenka et al.; 2016):

$$F_{3P}^p = \left[\sqrt{1.5}\frac{\rho}{f_c'}\right]^2 + m\left[\frac{\rho}{\sqrt{6}f_c'}r(\theta, e) + \frac{\xi}{\sqrt{3}f_c'}\right] - c = 0 \tag{2.6}$$

Where

$$m = 3\frac{f_c'^2 - f_t'^2}{f_c'f_t'}\frac{e}{e+1}$$

and

$$r(\theta, e) = \frac{4(1-e^2)\cos^2\theta + (2e-1)^2}{2(1-e^2)\cos\theta + (2e-1)[4(1-e^2)\cos^2\theta + 5e^2 - 4e]^{\frac{1}{2}}}$$

In the above equations, ξ, ρ, and θ are Haigh–Westergaard coordinates, and e is a parameter defining the roundness of the failure surface. The failure surface has a sharp corner

if $e = 0.5$ and is fully circular if $e = 1.0$.

The parameter c in equation 2.6 controls the hardening/softening, and evolves during the yielding/crushing process:

$$c = \left(\frac{f'_c(\varepsilon^p_{eq})}{f'_c} \right)^2 \tag{2.7}$$

Where the equivalent plastic strain, ε^p_{eq} is given by:

$$\Delta\varepsilon^p_{eq} = min(\Delta\varepsilon^p_{ij}) \tag{2.8}$$

2.6.3 Rankine-Fracturing model for Concrete Cracking

The Rankine criterion is used for concrete cracking:

$$F^f_i = \sigma'^t_{ii} - f'_{ti} \leq 0 \tag{2.9}$$

It's assumed that strains and stresses are converted into the material directions, which depends on the model. In the case of the rotated crack model, the material directions correspond to the principal directions, and in the case of the fixed crack model, they are given by the principal directions at the onset of cracking (Červenka et al.; 2016). σ'^t_{ii} identifies the trial stress, and f'_{ti} the tensile strength in the material direction i. The prime symbol denotes quantities in the different material directions. The trial stress state is computed by the elastic predictor:

$$\sigma'^t_{ij} = \sigma'^{n-1}_{ij} + E_{ijkl}\Delta\varepsilon'_{kl} \tag{2.10}$$

If the trial stress does not satisfy equation 2.9, the increment of fracture strain in direction i can be calculated using the assumption that the final stress state must satisfy equation 2.11:

$$F^f_i = \sigma'^n_{ii} - f'_{ti} = \sigma'^t_{ii} - E_{ijkl}\Delta\varepsilon'^f_{kl} - f'_{ti} = 0 \tag{2.11}$$

Equation 2.11 can be further simplified under the assumption that the fracture strain increment is normal to failure surface, and that only one failure surface is checked. For failure surface k, the fracture strain increment then has the following form:

$$\Delta\varepsilon'^f_{ij} = \Delta\lambda\frac{\partial F^f_k}{\partial\sigma_{ij}} = \Delta\lambda\delta_{ik} \tag{2.12}$$

After substituting into equation 2.11, an equation for the increment of the fracturing multiplier, λ, is recovered:

$$\Delta\lambda = \frac{\sigma'^t_{kk} - f'_{tk}}{E_{kkkk}} = \frac{\sigma'^t_{kk} - f'_t(w^{max}_k)}{E_{kkkk}}, \text{ and } w^{max}_k = L_t(\hat{\varepsilon}'^f_{kk} + \Delta\lambda) \tag{2.13}$$

This equation must be solved by iterations, as for softening materials, the value of current tensile strength, $f'_t(w^{max}_k)$, is a function of crack opening, w.

The crack opening, w, is calculated from the total value of fracturing strain, $\hat{\varepsilon}'^f_{kk}$, in direction k, plus the current increment of fracturing strain, $\Delta\lambda$. This sum is then multiplied with the characteristic length, L_t.

2.6.4 Combination of Plasticity and Fracture Model

As both the above models has to be used, we combine them into one - using plasticity for concrete crushing and the Rankine fracture model for cracking. The problem is stated as a simultaneous solution of the following inequalities (Červenka et al.; 2016):

$$F^p(^{(n-1)}\sigma_{ij} + E_{ijkl}(\Delta\varepsilon_{kl} - \Delta\varepsilon_{kl}^f - \Delta\varepsilon_{kl}^p)) \leq 0, \text{ solve for } \Delta\varepsilon_{kl}^p \qquad (2.14)$$

$$F^f(^{(n-1)}\sigma_{ij} + E_{ijkl}(\Delta\varepsilon_{kl} - \Delta\varepsilon_{kl}^p - \Delta\varepsilon_{kl}^f)) \leq 0, \text{ solve for } \Delta\varepsilon_{kl}^f \qquad (2.15)$$

2.6.5 Bond slip

The bond between steel bars and the concrete is an important part of the reinforced concrete mechanical system, and has been researched by many. Two of the available models are the one from Bigaj (1999), and the one from *FIB Model Code* (2010):

2.6.5.1 FIB Model Code

The bond law described by FIB Model Code 2010 is shown in figure 2.9. The bond is described by the set of given equations:

$$\begin{aligned}
\tau_{b0} &= \tau_{bmax}\left(\frac{s}{s_1}\right)^\alpha & \text{for } 0 \leq s \leq s_1 \\
\tau_{b0} &= \tau_{bmax} & \text{for } s_1 \leq s \leq s_2 \\
\tau_{b0} &= \tau_{bmax} - (\tau_{bmax} - \tau_{bf})\frac{s - s_2}{s_3 - s_2} & \text{for } s_2 \leq s \leq s_3 \\
\tau_{b0} &= \tau_{bmax} & \text{for } s_3 \leq s
\end{aligned} \qquad (2.16)$$

Where the parameters are given in table 2.1
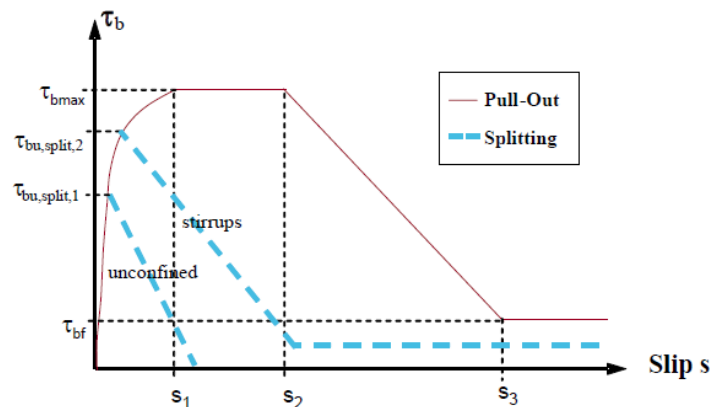
Figure 2.9: Bond Law according to FIB MC 2010 (*FIB Model Code*; 2010)

	Pull-Out (PO)		Splitting (SP)			
	$\varepsilon_s < \varepsilon_{sy}$		$\varepsilon_s < \varepsilon_{sy}$			
	Good bond cond.	All other bond cond.	Good bond cond.		All other bond cond.	
			unconfined	stirrups	unconfined	stirrups
τ_{bmax}	$2.5\sqrt{f_{cm}}$	$1.25\sqrt{f_{cm}}$	$7.0\left(\frac{f_{cm}}{25}\right)^{0.25}$	$8.0\left(\frac{f_{cm}}{25}\right)^{0.25}$	$5.0\left(\frac{f_{cm}}{25}\right)^{0.25}$	$5.5\left(\frac{f_{cm}}{25}\right)^{0.25}$
s_1	1.0mm	1.8mm	$s(\tau_{bmax})$	$s(\tau_{bmax})$	$s(\tau_{bmax})$	$s(\tau_{bmax})$
s_2	2.0mm	3.6mm	s_1	s_1	s_1	s_1
s_3	c_{clear}[1]	c_{clear}[1]	$1.2s_1$	$0.5c_{clear}$[1]	$1.2s_1$	$0.5c_{clear}$[1]
α	0.4	0.4	0.4	0.4	0.4	0.4
τ_{bf}	$0.4\tau_{bmax}$	$0.4\tau_{bmax}$	0	$0.4\tau_{bmax}$	0	$0.4\tau_{bmax}$

[1] c_{clear} is the clear distance between ribs.

Table 2.1: Parameters defining the mean bond stress-slip relationship of ribbed bars (according to eq. 2.16) (*FIB Model Code*; 2010)

The values for pull-out failure in table 2.1 are only valid for well confined concrete (cover $\geq 5\varnothing$, and clear spacing between bars $\geq 10\varnothing$).

2.6.5.2 Bigaj 1999

The bond law described in fig. 2.10 is based on the work from Bigaj (1999). This model depends on the bond quality, reinforcement diameter D, and the concrete cubic compressive strength, f'_{cu}.
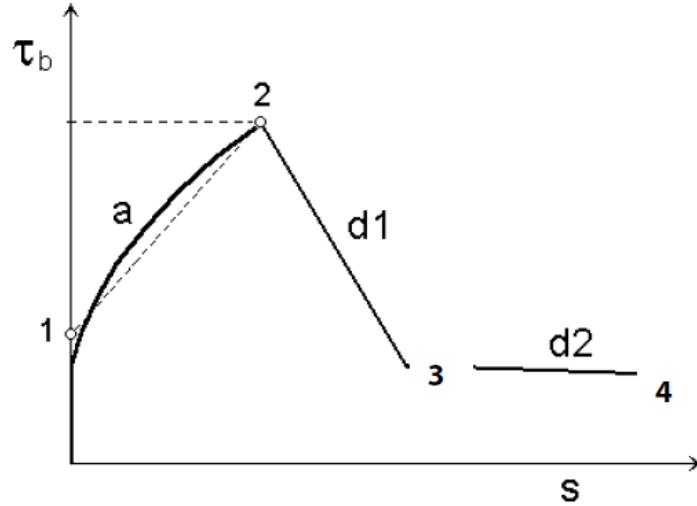
Figure 2.10: Bond Law according to Bigaj 1999 (Bigaj; 1999)

Concrete Type	Bond Quality		Point 1	Point 2	Point 3	Point 4
$f'_c < 60$	Excellent	s/D	0.000	0.020	0.044	0.480
		$\tau_b/\sqrt{0.8f'_{cu}}$	0.500	3.000	0.700	0.000
	Good	s/D	0.000	0.030	0.047	0.480
		$\tau_b/\sqrt{0.8f'_{cu}}$	0.500	2.000	0.700	0.000
	Bad	s/D	0.000	0.040	0.047	0.480
		$\tau_b/\sqrt{0.8f'_{cu}}$	0.500	1.000	0.700	0.000
$f'_c > 60$	Excellent	s/D	0.000	0.012	0.030	0.340
		$\tau_b/\sqrt{0.8f'_{cu}}$	0.600	2.500	0.900	0.000
	Good	s/D	0.000	0.020	0.030	0.340
		$\tau_b/\sqrt{0.8f'_{cu}}$	0.600	1.900	0.900	0.000
	Bad	s/D	0.000	0.025	0.030	0.340
		$\tau_b/\sqrt{0.8f'_{cu}}$	0.600	1.100	0.900	0.000

Table 2.2: Parameters for defining the bond strength-slip relationship for smooth bars according to Bigaj 1999 Bond Law (Červenka et al.; 2016).

3 Crack Width Calculations

3.1 EN 1992-1-1:2018

The crack width calculations based on EN 1992-1-1:2018 are calculated nominal values, and may differ from values measured on site.

The calculated surface crack width, $w_{k,cal}$, may be determined from equation 3.1:

$$w_{k,cal} = S_{r,max,cal}(\varepsilon_{sm} - \varepsilon_{cm} + \eta_r \varepsilon_{cs}) \tag{3.1}$$

Where:

$S_{r,max,cal}$	is the calculated maximum crack spacing when cracking is stabilized or alternatively the maximum length along which there is slip between concrete and steel in the phase of crack formation, and may me determined from equation 3.2
ε_{sm}	is the mean strain in the reinforcement closest to the most tensioned concrete surface under the relevant combination of actions, including the effect of imposed deformations and taking into account the effects of tension stiffening.
ε_{cm}	is the mean strain in the concrete between cracks at the same level of ε_{sm}.
η_r	is equal to 0 for short-term loading, and for long term loading in the crack formation phase.
ε_{cs}	is the shrinkage strain.

$$S_{r,max,cal} = \left(2c + 0.35 k_b \frac{\phi}{\rho_{p,ef}}\right) \cdot \left(1 - \frac{f_{Fts,ef}}{f_{ctm}}\right) \tag{3.2}$$

Where:

c	is the clear cover, i.e., the distance between the tensioned concrete surface and the outer edge of the longitudinal reinforcement closest to the concrete surface.
k_b	is a coefficient which takes account of the bond properties of the bonded reinforcement. It may be taken equal to: = 0,8 for ribbed and indented reinforcing steel bars or prestressing = 1,6 for bars with an effectively plain surface
ϕ	is the bar diameter. Where a mixture of bar diameters is used in a section, ϕ should be taken as the equivalent diameter.
$\rho_{p,ef}$	$= (A_s + \xi_1 A_p)/A_{c,eff}$
$f_{Fts,ef}$	is the effective residual tensile strength for the serviceability limit states $= \kappa_O \cdot \kappa_G \cdot \alpha_{t1} \cdot f_{R,1k}$, Where $\alpha_{t1} = 0.53 - 0.14 \cdot \frac{f_{R,3k}}{f_{R,1k}}$
f_{ctm}	is the mean axial tensile strength of concrete at age t_{ref}

The value $w_{k,cal}$ is to be compared with $w_{lim,cal}$, which for a quasi-permanent combination of actions for most exposure classes is equal to 0.3mm (*EN 1992-1-1:2018*; 2018)

3.2 fib Model Code 2010 / NB38

The crack width calculations specified in fib Model Code 2010 and NB38 are equal - and thus treated as one in the following section.
The design crack width w_d in FRC elements can be calculated by equation 3.3:

$$w_d = 2\left\{k \cdot c + \frac{1}{4}\frac{\phi_s}{\rho_{s_{ef}}} \cdot \frac{(f_{ctm} - f_{Ftsm})}{\tau_{bms}}\right\} \cdot \frac{1}{E_s} \cdot (\sigma_s - \beta \cdot \sigma_{sr} + \eta_r \cdot \varepsilon_{sh} \cdot E_s) \leq w_{lim} \quad (3.3)$$

Where:

k	is an empirical parameter to take the influence of the concrete cover into consideration; as a simplification, k = 1.0 can be assumed
c	is the concrete cover
ϕ_s	is the bar diameter used in the tensile zone
$\rho_{s,ef}$	$= \dfrac{A_s}{A_{c,ef}}$ With $A_{c,ef}$ = effective area of concrete in tension (Figure 3.1)
f_{ctm}	is the mean axial tensile strength of concrete
f_{Ftsm}	$= \dfrac{f_{Ftsk}}{0.7}$ where $f_{Ftsk} = 0.45 f_{R1k}$
τ_{bms}	is the mean bond strength between steel and concrete (Table 3.1)
E_s	is the design value of modulus of elasticity of ordinary reinforcing steel
σ_s	is the steel stress in a crack, including the effect of fibres (f_{Ftsm})
β	is an empirical coefficient to assess the mean strain over $l_{s,max}$ depending on the type of loading (Table 3.1)
σ_{sr}	is the maximum steel stress in a crack in the crack formation stage: $= (f_{ctm} - f_{Ftsm}) \cdot (1 + \alpha_e \rho_{s,ef})/\rho_{s,ef}$ α_e is the modular ratio $= \dfrac{E_s}{E_c}$
η_r	is a coefficient for considering the shrinkage contribution (Table 3.1)
ε_{sh}	is the shrinkage strain
w_{lim}	= 0.30mm for exposure classes XC, XD, XF, XS
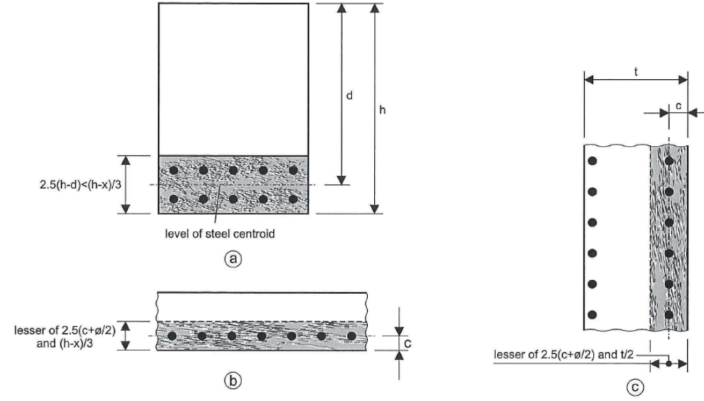
Figure 3.1: Effective tension area of concrete $A_{c,ef}$ for: (a) beam; (b) slab; (c) wall in tension (shaded areas) (*FIB Model Code*; 2010)

	Crack Formation Stage	**Stabilized cracking stage**
Short term, instantaneous loading	$\tau_{bms} = 1.8 \cdot f_{ctm}(t)$ $\beta = 0.6$ $\eta_r = 0$	$\tau_{bms} = 1.8 \cdot f_{ctm}(t)$ $\beta = 0.6$ $\eta_r = 0$
Long term, repeated loading	$\tau_{bms} = 1.35 \cdot f_{ctm}(t)$ $\beta = 0.6$ $\eta_r = 0$	$\tau_{bms} = 1.8 \cdot f_{ctm}(t)$ $\beta = 0.4$ $\eta_r = 1$

Table 3.1: Values for τ_{bms}, β and η_r for deformed reinforcing bars (*FIB Model Code*; 2010)

3.3 Comparison of crack-width calculations from FIB MC 2010, EN 1992, and NB38

In this thesis, the residual strength classes given in EN 1992-1-1:2018, Annex L, is used to compare the different guidelines. The table is given in tab. 3.2.

$f_{R,3k}/f_{R,1k}$	$f_{R,1k}$									
	1,0	**1,5**	**2,0**	**2,5**	**3,0**	**4,0**	**5,0**	**6,0**	**8,0**	**10,0**
a $(0.5 \leq f_{R,3k}/f_{R,1k} < 0.7)$ $f_{R,3k} = 0.5 f_{R,1k}$	0,5	0,8	1,0	1,3	1,5	2,0	2,5	3,0	4,0	5,0
b $(0.7 \leq f_{R,3k}/f_{R,1k} < 0.9)$ $f_{R,3k} = 0.7 f_{R,1k}$	0,7	1,1	1,4	1,8	2,1	2,8	3,5	4,2	5,6	7,0
c $(0.9 \leq f_{R,3k}/f_{R,1k} < 1.1)$ $f_{R,3k} = 0.9 f_{R,1k}$	0,9	1,4	1,8	2,3	2,7	3,6	4,5	5,4	7,2	9,0
d $(1.1 \leq f_{R,3k}/f_{R,1k} < 1.3)$ $f_{R,3k} = 1.1 f_{R,1k}$	1,1	1,7	2,2	2,8	3,3	4,4	5,5	6,6	8,8	11,0
e $(f_{R,3k}/f_{R,1k} \geq 1.3)$ $f_{R,3k} = 1.3 f_{R,1k}$	1,3	2,0	2,6	3,3	3,9	5,2	6,5	7,8	10,4	13,0

Table 3.2: Characteristic residual flexural strengths $f_{R,3k}$ for a given class (*EN 1992-1-1:2018*; 2018)

Example: The theoretical crack-width has been calculated for several classes from table 3.2, with results shown in fig. 3.4 The full calculations can be found in Appendix B. The calculations are based on the simply supported beam of length 5m given in fig. 3.2.
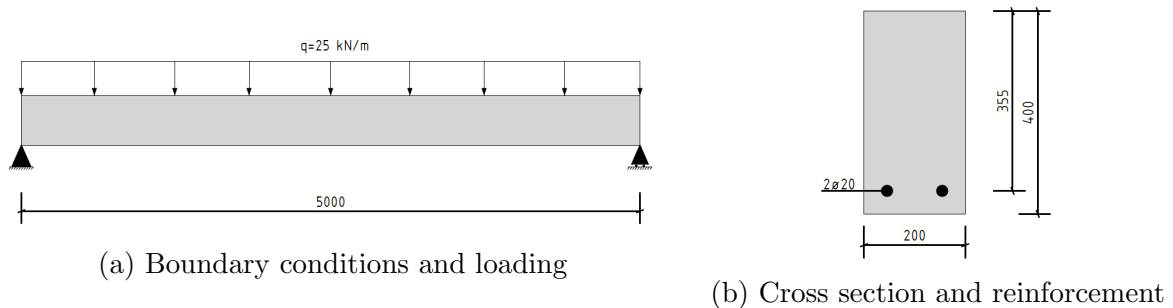

(a) Boundary conditions and loading

(b) Cross section and reinforcement

Figure 3.2: Beam used for crack-width calculations (dimensions in mm)

In order to calculate the crack widths, the stress in the longitudinal bars, σ_s, has to be determined. This can be obtained from the system of equilibrium equations of forces and moments. (Figure 3.3, Equations (3.4) to (3.8))
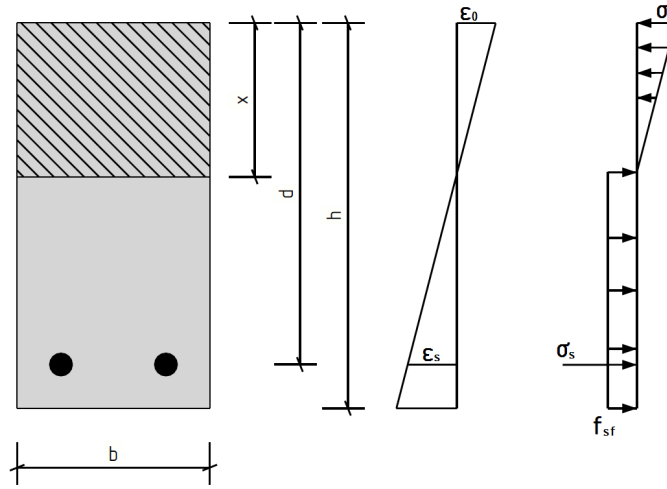

Figure 3.3: Strains and stresses on a cracked SFRC section in bending

The depth of the neutral axis, x, can be determined by considering force equilibrium. Unlike in plain RC members, an iterative process is needed in SFRC as the assumed stress carried by the fibres, f_{sf}, is independent on the induced strain. From equilibrium, it can be shown that:

$$x = \frac{E_s \varepsilon_s A_s + f_{sf} bh}{\frac{1}{2} E_c \varepsilon_0 b + f_{sf} b} \tag{3.4}$$

Taking the moment about the neutral axis of the fibre component gives the following internal resisting moment:

$$M = 0.5 \sigma_c bx(\frac{2}{3}x + \frac{h-x}{2}) + E_s \varepsilon_s A_s(d - x - \frac{h-x}{2}) \tag{3.5}$$

Assuming the loads are low enough not causing the steel to yield, the strain in the reinforcing bars can be taken as:

$$\varepsilon_s = \frac{d-x}{x} \varepsilon_0 \tag{3.6}$$

Substituting equation 3.6 into equation 3.5 gives us the following solution for ε_0:

$$\varepsilon_0 = \frac{M}{0.5 E_c bx(\frac{h}{2} + \frac{x}{6}) + E_s A_s(\frac{d-x}{x})(d - \frac{x}{2} - \frac{h}{2})} \tag{3.7}$$

For a given moment, a trial neutral axis is chosen (e.g. $0.45d$). Solving eq. 3.7 gives the extreme concrete compressive fibre strain, ε_0, which is then used in equation 3.6 to solve for the strain in the reinforcement. During this step, it is necessary to check whether or not the steel strain is below yield ($\varepsilon_s \leq \varepsilon_{sy} = f_{sy}/E_s$). Finally solving for x in equation 3.4 will check the initial assumption of x, and if required, x is iterated until convergence. With x converged, σ_s is finally calculated as:

$$\sigma_s = E_s \varepsilon_s = E_s \frac{d-x}{x} \varepsilon_0 \tag{3.8}$$

A Matlab code was developed during the work of the thesis in order to solve the iterative calculations, see appendix C, p. k.
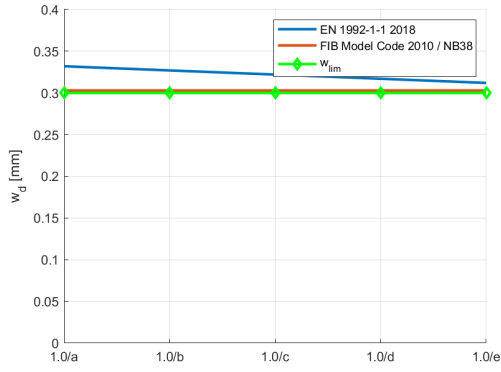
(a) Class 1.0
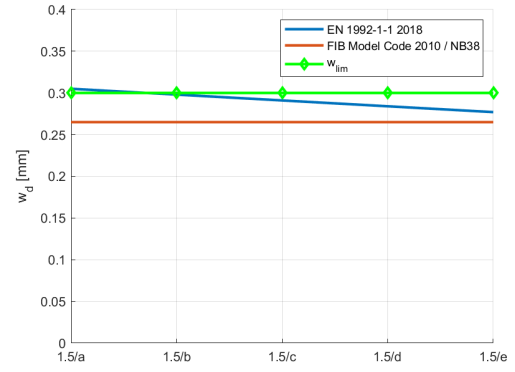
(b) Class 1.5

(c) Class 2.0

(d) Class 2.5

(e) Class 3.0
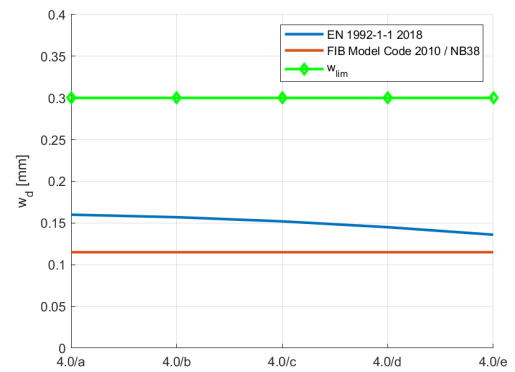
(f) Class 4.0

Figure 3.4: w_d of section shown in fig. 3.2 with increasing flexural strengths $f_{R,1k}$ and $f_{R,3k}$

As can be seen, FIB MC 2010 and NB38 overestimates the contribution of the fibres compared to EN 1992-1-1:2018 - especially at low ratios of $\frac{f_{R,3k}}{f_{R,1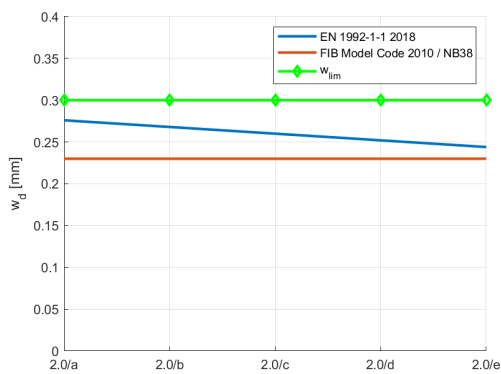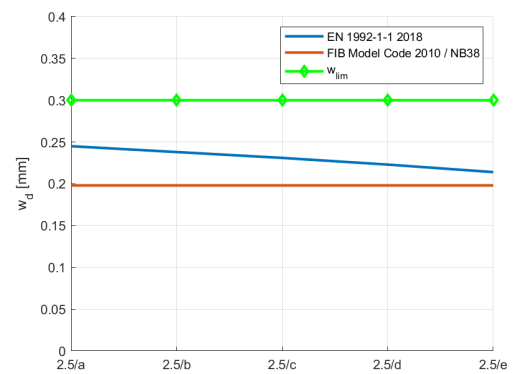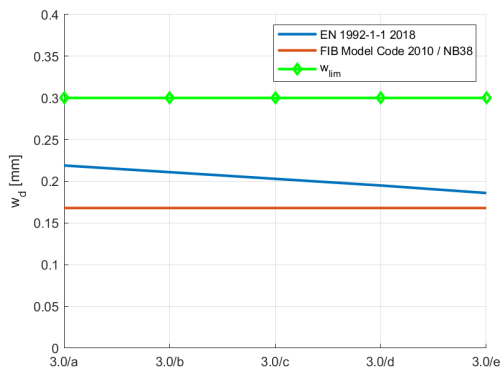k}}$ (class a, fig. 3.6). It is also noted that the crack width from FIB MC 2010 and NB38 are independent of $f_{R,3k}$, which is clearly visible in eq. (3.3):

$$w_{d,FIB,NB} = f(..) + f(f_{Ftsm}, \sigma_s) = f(..) + f(f_{Ftsm}) = f(..) + f(f_{R,1k}) \qquad (3.9)$$

i.e. FIB MC 2010 and NB38 neglects the change in residual flexural strength from $CMOD_1$ to $CMOD_3$ (fig. 3.5). This results in calculations neglecting the fact that the residual flexural strength may increase or decrease after the first cracks appear. This is especially important for class a and b, where the residual flexural strengths at $CMOD_3$ is respectively half, and 0.7 times the residual flexural strength at $CMOD_1$. The fact that FIB MC 2010 and NB38 neglects this may result in calculated crack-widths much lower than the actual values. On the other hand, for class d and e, the calculations may give conservative values for crack widths, as the fact that the residual flexural strength increases from $CMOD_1$ to $CMOD_3$ is neglected.

Figure 3.5: Change in residual flexural strength from $CMOD_1$ to $CMOD_3$ for class a to e

(a) Class a

(b) Class e

Figure 3.6: w_d of class a and e

The maximum final crack spacing, $S_{r,max}$, from the different guidelines is given as:
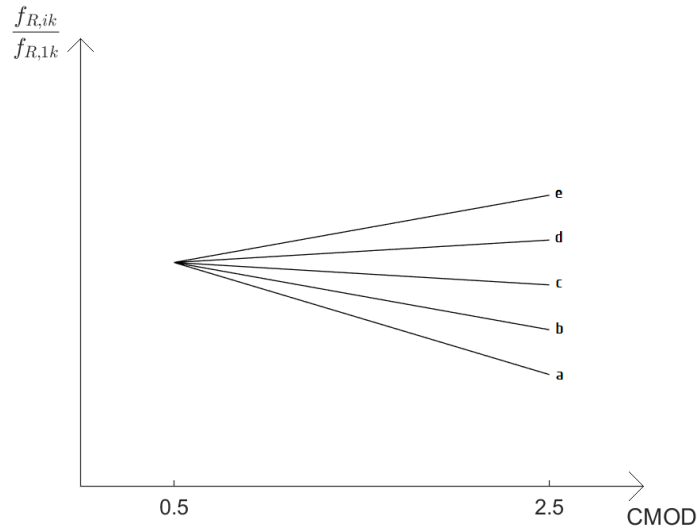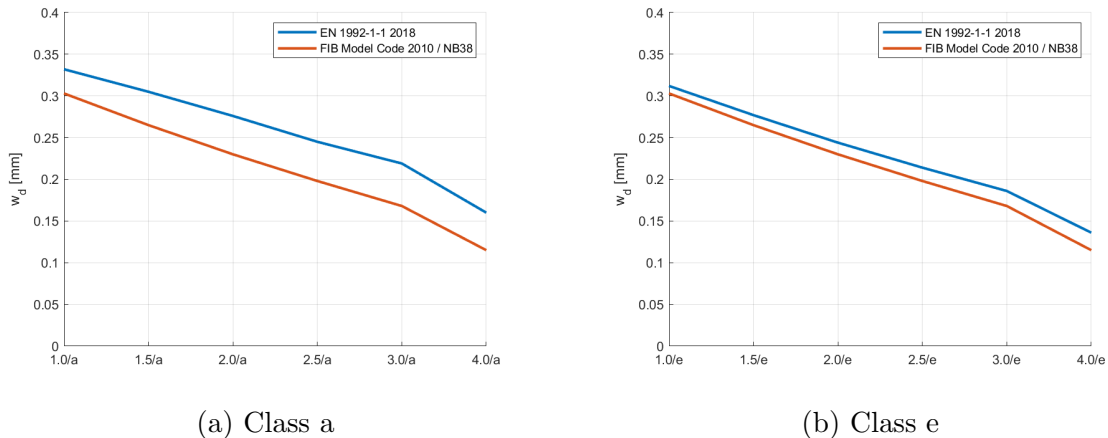
$$S_{r,max,EN} = (2c + 0.35k_b \frac{\phi}{\rho_{p,ef}}) \cdot (1 - \frac{f_{Fts,ef}}{f_{ctm}}) \quad (3.10)$$

$$S_{r,max,FIB,NB} = 2\left\{k \cdot c + \frac{1}{4}\frac{\phi_s}{\rho_{s_{ef}}} \cdot \frac{(f_{ctm} - f_{Ftsm})}{\tau_{bms}}\right\} \quad (3.11)$$

Comparing them, we can see that in FIB MC 2010 and NB38 the clear distance, c, part of the equation is not influenced by f_{Ftsm}, and thus if f_{Ftsm} is set equal to f_{ctm} we obtain:

$$S_{r,max,FIB,NB} = 2kc \quad (3.12)$$

In the equation from EN 1992-1-1:2018 the situation is different, and if $f_{fts,ef}$ is set equal to f_{ctm} we obtain:

$$S_{r,max,EN} = 0 \quad (3.13)$$

Increasing f_{fts} further will thus make $s_{r,max,EN}$ negative for values $> f_{ctm}$, while $s_{r,max,FIB,NB}$ stays positive until:

$$f_{Ftsm} > \frac{4 \cdot k \cdot c \cdot \rho_{s,ef} \cdot \tau_{bms}}{\phi_s} + f_{ctm} \quad (3.14)$$

It is noted that at the time of delivery of this thesis, the group designing Annex L for EN 1992-1-1:2018 are still debating which residual tensile strength that should be used in the $S_{r,max}$ calculation (Kanstad; 2019).

A comparison of the calculated mean crack spacing from EN 1991-1-1.2018 and measured values has been carried out by the task group designing Annex L, showing how the equation compare to measured values. The results are shown in fig. 3.7, and show that for a given calculated crack spacing, a vast difference in measured crack spacings can be seen.
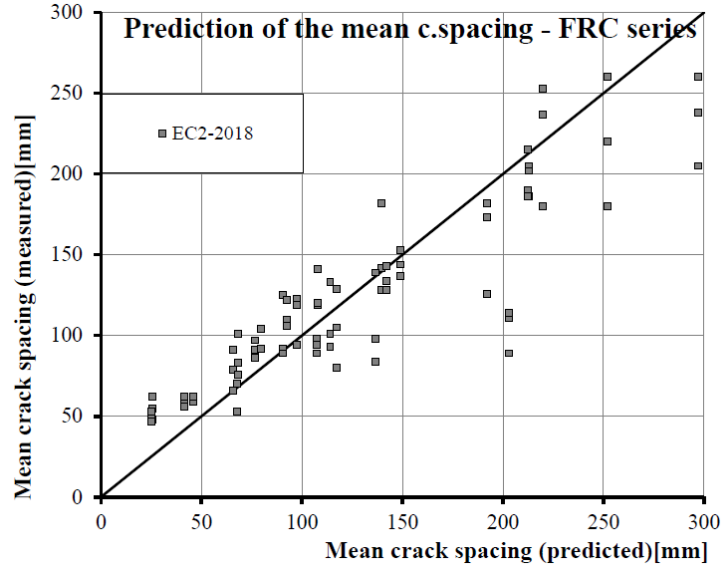

Figure 3.7: Measured vs. calculated mean crack spacing (Plizzari; 2019)

4 Shear Capacity Calculations

In the following sections, shear capacity calculations are described, and carried out for a beam without shear reinforcement. Formulas for members requiring shear reinforcement are nevertheless included in the thesis, merely to illustrate the differences between the guidelines.

4.1 EN 1992-1-1:2018

The shear capacity of a concrete section $V_{Rd} = \tau_{Rd} b_w d$ where τ_{Rd} depends on the reinforcement. (Equation 4.1 or 4.3)

NB: The calculations based on EN 1992-1-1:2018 are <u>**not**</u> to be used for structural design at the time of this thesis being published, as they currently are being controlled. The author and the suppliers of the draft of EN 1992-1-1:2018 take no responsibility for any structural use of them before the official release in mid. 2020.

4.1.1 Members not requiring design shear reinforcement

$$\tau_{Rd,cF} = \frac{0.6}{\eta \cdot \gamma_c}(100\rho_l f_{ck}\frac{d_{dg}}{d})^{1/3} + f_{Ftud} \geq \tau_{Rdc,min} + f_{Ftud} \tag{4.1}$$

Where:

η	is a parameter which expresses that the two contributions are not additive $= min(1 + 0.43f_{Ftud}^{2.85}; 2.5)$
γ_c	is the partial factor of safety for concrete
ρ_l	$= \dfrac{A_{sl}}{b_w d}$
A_{sl}	is the area of the tensile reinforcement, which extends $\geq (l_{bd} + d)$ beyond the section considered
d_{dg}	is a size parameter describing the failure zone roughness, taking into account the concrete type and its aggregate properties. Its value may be taken as: $16 + D_{lower} \leq 40$ [mm] for concrete with $f_{ck} \leq 60$ MPa $16 + D_{lower}(60/f_{ck})^2 \leq 40$ [mm] for concrete wtih $f_{ck} \geq 60$ MPa
f_{Ftud}	$= f_{Ftu,ef}/\gamma_{sf}$
$f_{Ftu,ef}$	$= \kappa_O \cdot \kappa_G \cdot f_{Ftuk}$
f_{Ftuk}	$= \alpha_{t3} \cdot f_{R,3k}$
α_{t3}	$= 0.57 - 0.26f_{R,1k}/f_{R,3k}$
κ_O	is a factor accounting for fibre orientation $= 1.0$ (to be discussed before final release of EN 1992-1-1:2018)
κ_G	is a factor accounting for volume effects $= 1.0 + A_{ct} \cdot 0.5 \leq \kappa_{G,max} = 1.5$
A_{ct}	is the involved tension zone in the concrete of the cracked cross-sections of an equilibrium system in m^2

The value for $\tau_{Rdc,min}$ will be coordinated with the method for structures with fibres only at a later version of EN 1992-1-1:2018, but at the time, $\tau_{Rdc,min}$ is taken as:

$$\tau_{Rdc,min} = \frac{10}{\gamma_c}\sqrt{\frac{f_{ck}}{f_{yd}} \cdot \frac{d_{dg}}{d}} \tag{4.2}$$

4.1.2 Members requiring design shear reinforcement

For FRC members with design shear reinforcement, steel fibres, and longitudinal bars in the tensile zone, the design value of the shear stress resistance in [MPa] should be determined by equation 4.3. The equation is still to be verified (*EN 1992-1-1:2018*; 2018).

$$\tau_{Rd,sF} = (\kappa_s \frac{A_{sw}}{s} \frac{z}{b_w d} f_{yd} + \kappa_F f_{Ftud}) \tag{4.3}$$

Where:

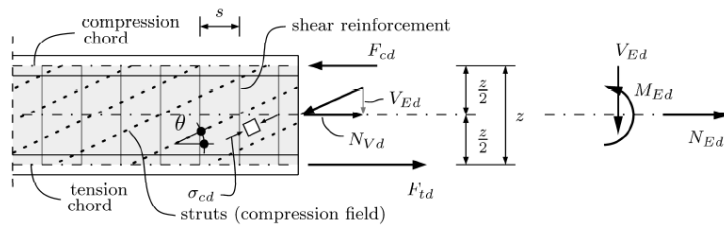|	
κ_s	$= 0.75$
κ_F	$= 1.0$
A_{sw}	is the cross sectional area of the shear reinforcement
s	is the spacing of the shear reinforcement in [mm]
z	is the internal lever arm, which for the shear calculation may be assumed as $0.9d$ (Figure 4.1)

Figure 4.1: Model and notation for shear reinforced members (*EN 1992-1-1:2018*; 2018)

4.2 fib Model Code 2010

4.2.1 Beams without shear reinforcement

The design value for the shear resistance in members with conventional longitudinal reinforcement and without shear reinforcement is given by equation 4.4:

$$V_{Rd,F} = \left\{ \frac{0.18}{\gamma_c} \cdot k \cdot \left[100 \cdot \rho_l \cdot \left(1 + 7.5 \cdot \frac{f_{Ftuk}}{f_{ctk}} \right) \cdot f_{ck} \right]^{1/3} + 0.15 \cdot \sigma_{cp} \right\} \cdot b_w \cdot d \geq V_{Rd,Fmin} \quad (4.4)$$

Where:

γ_c	is the partial factor of safety for the concrete without fibres
k	is a factor that takes into account the size effect and is equal to: $1 + \sqrt{\frac{200}{d}} \leq 2.0$
d	is the effective depth of the cross section in [mm]
ρ_l	is the longitudinal reinforcement ratio: $\rho_l = A_{sl}/(b_w d)$
A_{sl}	is the cross sectional area of the reinforcement which extends $\geq l_{bd} + d$ beyond the considered section [mm^2]
f_{Ftuk}	is the characteristic value of the ultimate residual tensile strength for FRC, by considering $w_u = 1.5$mm according to equation 4.5
f_{ctk}	is the characteristic value of the tensile strength for the concrete without fibres
f_{ck}	is the characteristic value of cylindrical compressive strength
σ_{cp}	$= N_{Ed}/A_c < 0.2 f_{cd}$ [MPa] is the average stress acting on the concrete cross section A_c [mm^2] for an axial force N_{Ed} [N], due to loading or prestressing actions ($N_{Ed} > 0$ for compression)
b_w	is the smallest width of the cross-section in the tensile area
$V_{Rd,Fmin}$	$= (v_{min} + 0.15 \cdot \sigma_{cp}) b_w d$ where: $v_{min} = 0.035 \cdot k^{3/2} \cdot f_{ck}^{1/2}$

$$f_{Ftu} = f_{Fts} - \frac{w_u}{\text{CMOD}_3}(f_{Fts} - 0.5 f_{R3} + 0.2 f_{R1}) \geq 0 \qquad (4.5)$$

$$f_{Fts} = 0.45 f_{R1} \qquad (4.6)$$

4.2.2 Beams with shear and longitudinal reinforcement

For FRC elements with shear reinforcement, the shear resistance is given by equation 4.7:

$$V_{Rd} = V_{Rd,F} + V_{Rd,s} \tag{4.7}$$

Where:

$V_{Rd,F}$	Follows from equation 4.4
$V_{Rd,s}$	Follows from equation 4.8

$$V_{Rd,s} = \frac{A_{sw}}{s_w} z f_{ywd} cot\theta \tag{4.8}$$

Where:

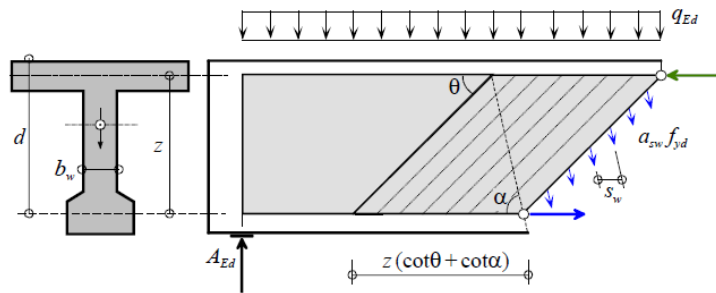|	
A_{sw}	is the area of the shear reinforcement
s_w	is the spacing of the shear reinforcement
z	is the effective shear depth $= 0.9d$
f_{ywd}	is the design yield strength of the shear reinforcement
θ	denotes the inclination of the compressive stress field (Figure 4.2)
	$30° < \theta < 45°$ (*FIB Model Code*; 2010)

Figure 4.2: Geometry and definitions of shear reinforcement (*FIB Model Code*; 2010)

4.3 NB38

The shear resistance calculations in NB38 may be regarded as a combination of the ones found in EN 1992-1-1 2004 and fib Model Code 2010. The shear resistance for a cross section without shear reinforcement is given by equation 4.9:

$$V_{Rd,c} = V_{Rd,ct} + V_{Rd,cf} \tag{4.9}$$

Where:

$V_{Rd,ct}$ is the shear force capacity from the concrete, and follows from equation 4.10
$V_{Rd,cf}$ is the shear force capacity from the fibres, and follows from equation 4.11

$$V_{Rd,ct} = \left[C_{Rd,c} \cdot k \cdot \left(100\rho_l f_{ck} \right)^{1/3} + k_1 \cdot \sigma_{cp} \right] \cdot b_w \cdot d \geq (v_{min} + k_1 \cdot \sigma_{cp}) \cdot b_w \cdot d \tag{4.10}$$

Where:

$C_{Rd,c}$ $= \frac{k_2}{\gamma_c}$ where $k_2 = 0.18$ for concrete with $D_{upper} \geq 16mm$ and where the coarse aggregate makes up $\geq 50\%$ of the total aggregates

k $= 1 + \sqrt{\frac{200}{d}} \leq 2.0$

ρ_l is the longitudinal reinforcement ratio:
$\rho_l = A_{sl}/(b_w d)$

k_1 $= 0.15$ for compression and $= 0.3$ for tension.

σ_{cp} $= N_{Ed}/A_c < 0.2f_{cd}$ [MPa] is the average stress acting on the concrete cross section A_c [mm²] for an axial force N_{Ed} [N], due to loading or prestressing actions ($N_{Ed} > 0$ for compression)

v_{min} $= 0.035 \cdot k^{2/3} \cdot f_{fck}^{1/2}$

$$V_{Rd,cf} = 0.6 \cdot f_{ftd,res,2.5} \cdot b_w \cdot d \tag{4.11}$$

Where:

$f_{ftd,res,2.5}$ $= \frac{f_{ftk,res,2.5}}{\gamma_{sf}}$ where $f_{ftk,res,2.5} = 0.37 \cdot f_{Rk,3}$

4.4 Comparison of shear resistance calculations from FIB MC 2010, EN 1992, and NB38

The results shown in fig. 4.4 are based on the cross section shown in fig. 4.3 with data shown in table 4.1. Calculations are shown in appendix A. As the characteristic residual strength depends on the fibre-matrix bond strength, which is usually a function of the concrete compressive strength as well as the fibre content, it may be unrealistic to specify a high value of $f_{R,1k}$ and $f_{R,3k}$ for a relatively low value of f_{ck}. This is disregarded in the following calculations - and it is noted that the calculations are *purely* theoretical.

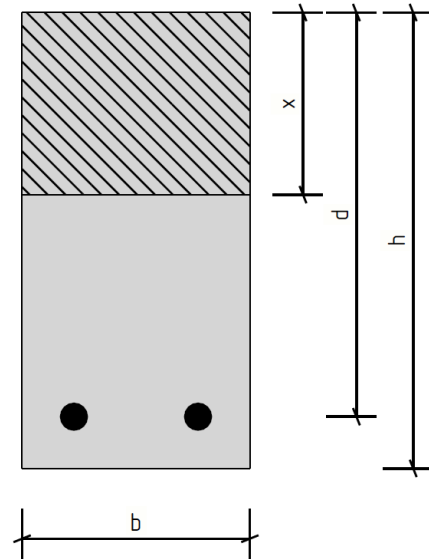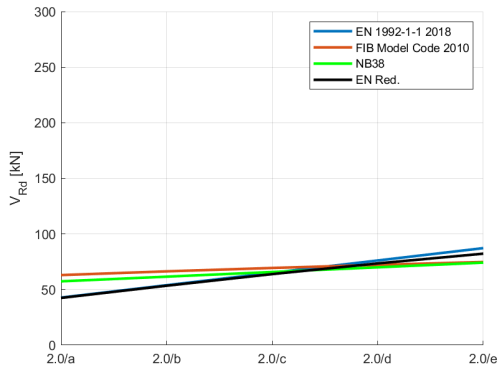| Concrete class	B35
f_{ck}	35 MPa
f_{ctm}	3.2 MPa
f_{ctk}	2.2 MPa
f_{yk}	500 MPa
γ_{sf}	1.5
γ_c	1.5
γ_s	1.15
ϕ_l	20mm
c_{nom}	35mm
D_{lower}	16mm
h	400mm
b	200mm
d	$= h - c_{nom} - \frac{\phi_l}{2} = 355$mm
x	See eq. (3.4)

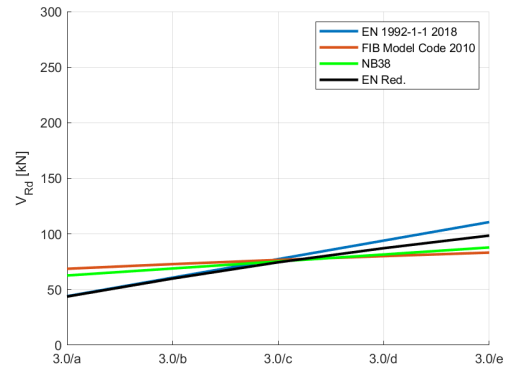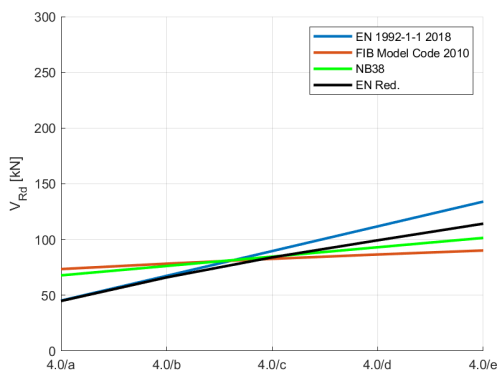Table 4.1: Data used in shear calculations

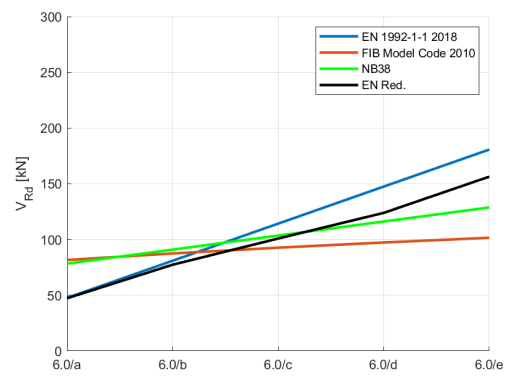Figure 4.3: Cross section of beam used in shear calculations
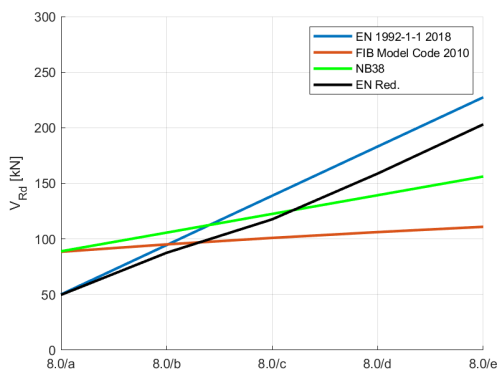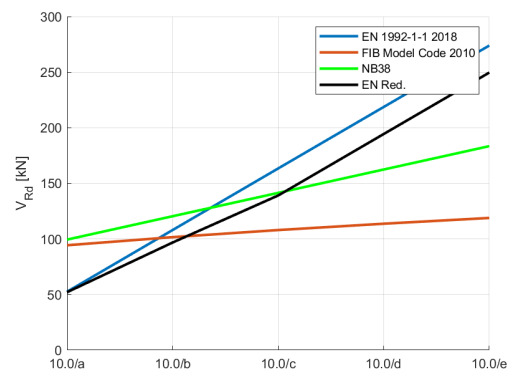
(a) Class 2.0

(b) Class 3.0

(c) Class 4.0

(d) Class 6.0

(e) Class 8.0

(f) Class 10.0

Figure 4.4: V_{Rd} of section shown in fig. 4.3 with increasing flexural strengths $f_{R,1k}$ and $f_{R,3k}$

As can be seen, EN 1992-1-1 dramatically overestimates the contribution of the fibres compared to FIB Model Code 2010 and NB38 when $f_{R,1k}$ and $f_{R,3k}$ increases. In the figures on the previous page, additional to the calculations from EN, FIB, and NB, a fourth result is shown, namely EN Red., calculated following eq. (4.1), but neglecting the minimum shear resistance. In order to compare the different guidelines, the factor a is introduced - a measure of the fibre contribution to the shear resistance: (It should be noted that the calculated a factors not necessarily represents the calculated shear resistance shown in fig. 4.4, as the a factor neglects the minimum shear resistance given in eqs. (4.1), (4.4) and (4.9).)

$$\frac{0.18}{\gamma_c} \cdot k \cdot \left(100\rho_l \left(1 + 7.5 \cdot \frac{f_{ftuk,fib}}{f_{ctk}}\right) f_{ck}\right)^{1/3} = \frac{0.6}{\eta\gamma_c}\left(100\rho_l f_{ck}\frac{d_{dg}}{d}\right)^{1/3} + a_{fib} \cdot f_{ftuk,EN} \quad (4.12)$$

Where $f_{ftuk,fib}$ is the characteristic value of the ultimate residual tensile strength taken from eq. (4.4), and $f_{ftuk,EN}$ is taken from eq. (4.1).

Solving for a_{fib} gives: (Complete formula attached in appendix D)

$$a_{fib} = f(d, d_g, f_{ck}, \rho_l, \eta, k, f_{ctk}, f_{ftuk,fib}, f_{ftuk,EN}) \quad (4.13)$$

Inputing the data from table 4.1 gives:

$$a_{fib} \approx -\frac{26259.0 \cdot \eta \cdot (6.3355 \cdot f_{R,1k} + 31.677 \cdot f_{R,3k} + 30.973)^{1/3} - 70405.0}{\eta \cdot (32500.0 \cdot f_{R,1k} - 71250.0 \cdot f_{R,3k})} \quad (4.14)$$

The factor a in EN 1992-1-1:2018 is given as:

$$a_{EN} = \frac{\kappa_O \cdot \kappa_G}{\gamma_{sf}} = \frac{1.0 \cdot min(1.0 + A_{ct} \cdot 0.5; 1.5)}{\gamma_{sf}} \quad (4.15)$$

Comparing eq. (4.9) and eq. (4.1) gives a for NB38 as:

$$a_{NB} \approx -\frac{16493.0 \cdot \eta + 3700.0 \cdot \eta \cdot f_{R,3k} - 14081.0}{\eta \cdot (6500.0 \cdot f_{R,1k} - 14250.0 \cdot f_{R,3k})} \quad (4.16)$$

The complete solution of a_{NB} is given in appendix E.

We can now compare the magnitude of the fibre contribution from the different guidelines by comparing the different guidelines a factor:

$$\tau_f = a \cdot f_{ftuk,EN} = a \cdot \left(0.57 - 0.26\frac{f_{R,1k}}{f_{R,3k}}\right) \cdot f_{R,3k} \quad (4.17)$$

Giving the magnitude of the fibre contribution for the shear resistance as:

$$\tau_f = a \cdot \left(0.57 \cdot f_{R,3k} - 0.26 \cdot f_{R,1k}\right) \quad (4.18)$$

On the next page, the a factor is plotted against class, showing how the different guidelines emphasize the fibre contribution as $f_{R,1k}$ and $f_{R,3k}$ change.
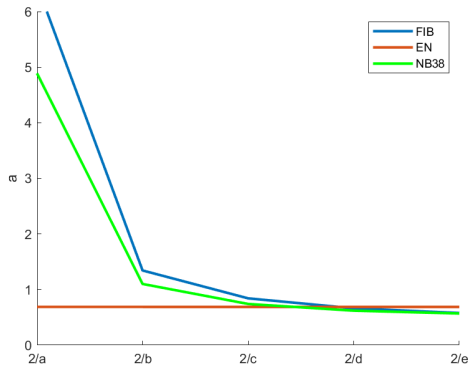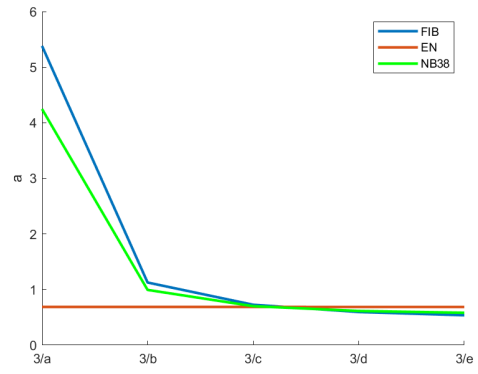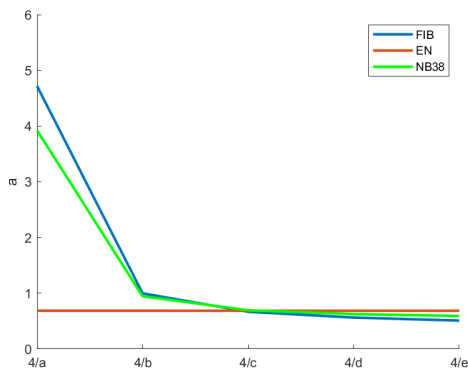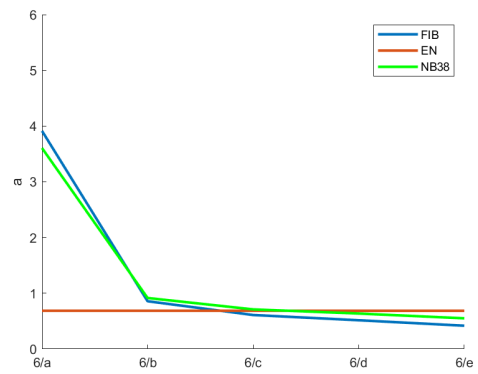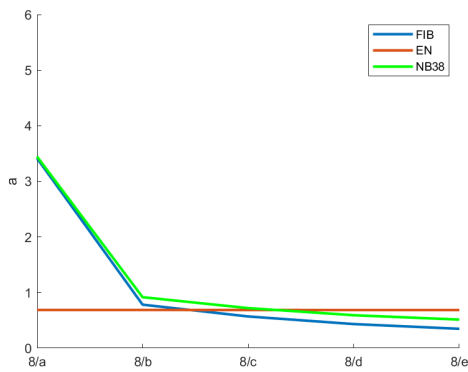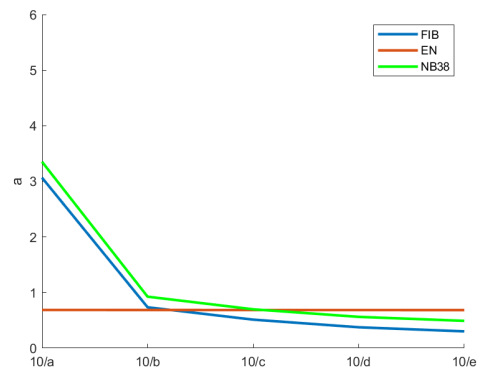
Figure 4.5: Comparison of variable a of section shown in fig. 4.3 with increasing flexural strengths $f_{R,1k}$ and $f_{R,3k}$

From these figures the varying degree of contribution from the fibres to the shear resistance can be read, and it's apparent that while EN 1992-1-1:2018 emphasizes the effect of the fibres more or less the same regardless of the residual flexural strengths $f_{R,1k}$ and $f_{R,3k}$, FIB Model Code 2010 and NB38 emphasize the effect at low values of $f_{R,3k}$, i.e. class a and b, and reduce the influence at higher values, i.e. class d and e. How these results agree with the results from finite element analyses will be further investigated in chapter 5.

5 Finite Element Modeling

A dapped end beam was modelled and analysed in order to investigate the shear capacity of the concrete. Two bars with ϕ=6mm is chosen to carry the tensile stresses appearing in the dapped end (as well as providing shear resistance by dowel effects, ref section 2.4). Two bars with ϕ=20mm is chosen to take the bending stress at the bottom of the beam in order to provoke a shear failure, and not a failure due to tensile stresses at the bottom of the beam.

5.1 Finite Element Model

The software used in the finite element modeling and analysis is Atena, developed by Cervenka Consulting.

5.2 Geometry

The geometry of the beam is given in figure 5.1 and the boundary conditions given in figure 5.2. The reinforcement is given in figure 5.3
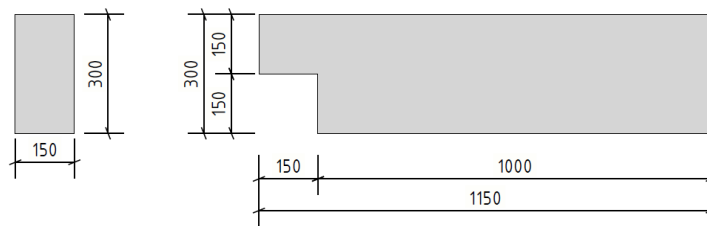
Figure 5.1: Geometry of the beam (Dimensions in mm)
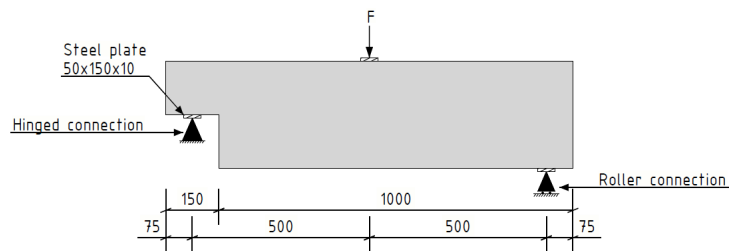
Figure 5.2: Test setup, including boundary conditions (Dimensions in mm)
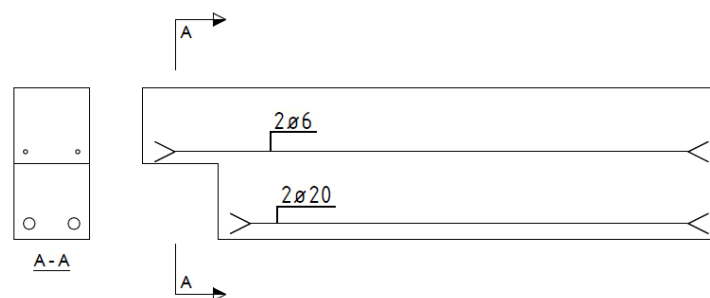
Figure 5.3: Reinforcement of the beam

5.2.1 Geometry

The geometry is modelled by first creating the lines defining the top- and bottom surface of the beam in the x-y plane, before extruding these in the z-plane to define the top and bottom surfaces. These surfaces are then respectively copied 0.15m in the negative and positive y-direction to form two dependent volumes. This is done in order to use a structured mesh (see section 5.2.4).

Next, the steel plates are defined in the same manner as the beam. The structural reinforcement in figure 5.3 is modelled as straight lines, and they will in section 5.3.2 be given an area and other parameters.

a) Lines defining top and bottom surface
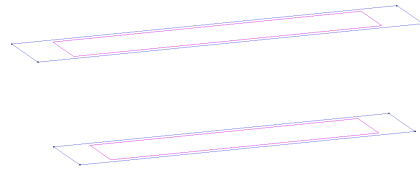
b) Top and bottom surfaces
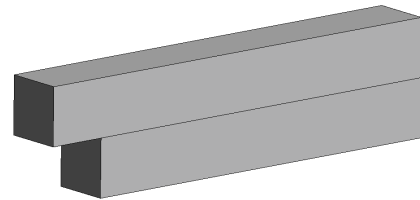
c) Volumes extruded
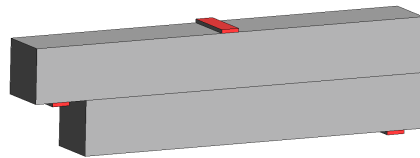
d) Steel plates added
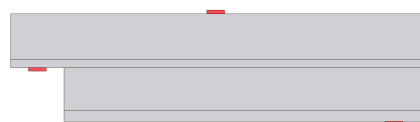
e) Reinforcement added

Figure 5.4: Development of FEM model

5.2.2 Boundary Conditions

The boundary conditions are modelled as described in fig. 5.2, including a boundary condition at the surfaces in the z-direction, to prevent abnormal behaviour.

(a) Boundary conditions at supports

(b) Boundary conditions of surfaces
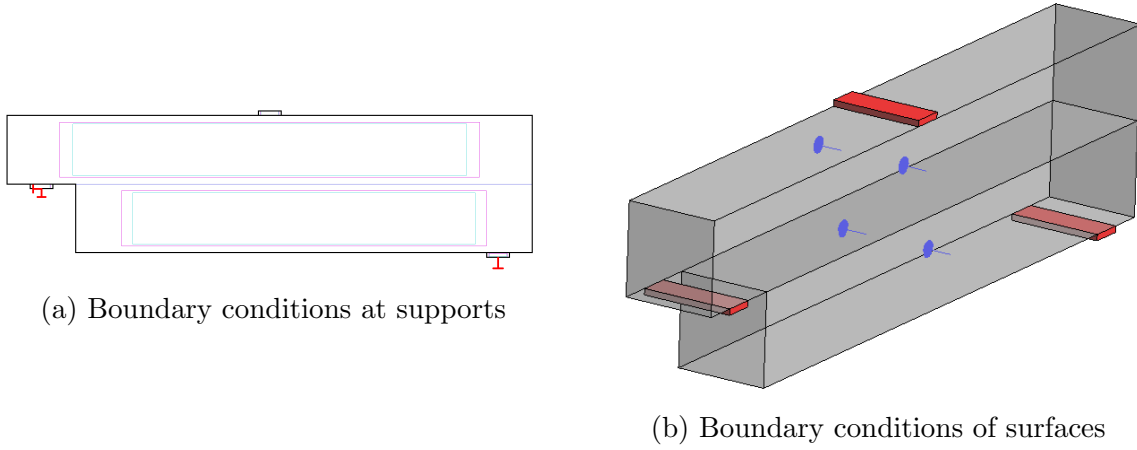
Figure 5.5: Boundary conditions of FEM-beam

5.2.3 Loading

In Atena, loading is recommended to be modelled as displacement-controlled, as opposed to force-controlled, which may scale the results (Červenka et al.; 2016). The loading is therefore modelled as a fixed starting displacement of $\delta_y = -0.1mm$. The maximum loading is assumed to occur in the range $-14mm \leq \delta_y \leq 0mm$, and the interval multiplier is thus set to 140, with a numerical evaluation for each step.
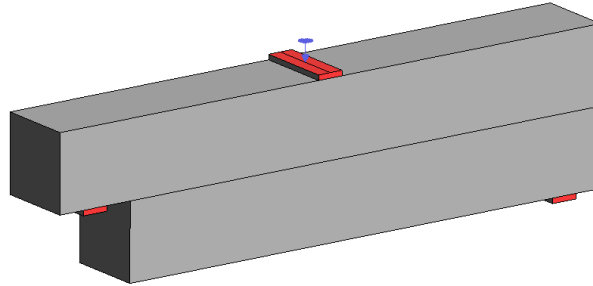
Figure 5.6: Loading of the beam

5.2.4 Meshing

It is suggested by Atena theory to use a structured mesh of quadratic hexahedral elements (fig. 5.7), as a mesh of tetrahedral elements gets less accurate when integrating the shape functions, and the computing power associated with tetrahedral elements is drastically larger than that of hexahedral ones (Benzley et al.; 1995). A structured mesh of size 0.025m is chosen, and later used as the characteristic tension size of the section. The final mesh can be seen in fig. 5.8.
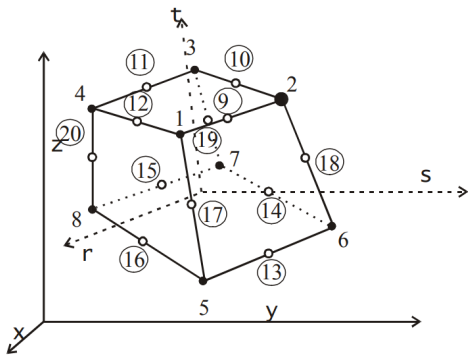
Figure 5.7: The quadratic hexahedral element (Červenka et al.; 2016)
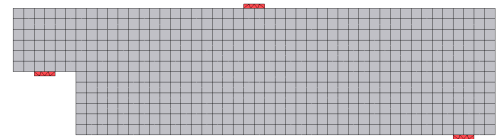
Figure 5.8: Mesh of the beam

5.3 Material Models

5.3.1 Concrete

The concrete is assigned the material model CC3DNonLinCementitious2User, a model based on the theories from chapter 2.6, p. 8, with a hardening regime before the compressive strength is reached (Figure 5.9). The material model allows for user defined tensile and softening behaviour. Input variables are listed in table 5.1.

Material name		Cementitious2 User	
Material Prototype		CC3DNonLinCementitious2User	
Young's modulus	E_{cm}	34	GPa
Poisson's ratio	ν	0.2	
Tensile strength	f_{ctk}	2.2	MPa
Compressive strength	f_{ck}	-35	MPa
Tension Characteristic size		0.025[a]	m
Tension Function		See section 5.3.1.1	
Aggregate size	D_{lower}	0.016	m
Compressive Function		See section 5.3.1.2	

[a] The tension characteristic size is set equal to the mesh size, see section 5.2.4.

Table 5.1: Input parameters for the SFRC
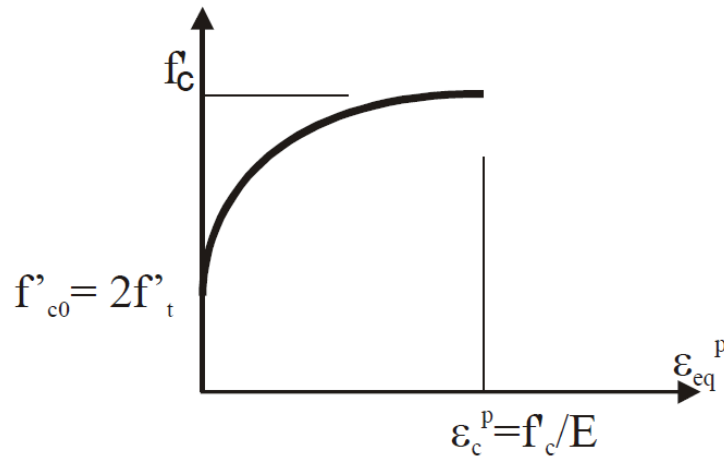
Figure 5.9: Compressive hardening/softening (Červenka et al.; 2016)

5.3.1.1 Tension Function

The tension function describes how the concrete behaves while under tensile stresses, i.e. how the tensile strength changes with the crack-width. The function is described as a set of points (ref. fig. 5.10) where:

$f_t = f_{ctk}$

σ_t is the residual tensile strength at w_c

$\varepsilon_f = \frac{w_c}{L_t}$ where w_c is the crack opening (CMOD) and L_t is the characteristic length, equal to the size of the element. For each class, five points are described:

	Point 1	Point 2	Point 3	Point 4	Point 5
ε_f	0.000	0.0001	$\frac{CMOD_1}{L_t} = \frac{0.5}{25} = 0.02$	$\frac{CMOD_3}{L_t} = \frac{2.5}{25} = 0.1$	0.3
$\frac{\sigma_t}{f_t}$	1.0	$\frac{0.45 f_{R,1k}}{f_{ctk}}$	$\frac{0.45 f_{R,1k}}{f_{ctk}}$	$\frac{0.37 f_{R,3k}}{f_{ctk}}$	0

Table 5.2: Points describing the tensile function of the FRC FEM-section
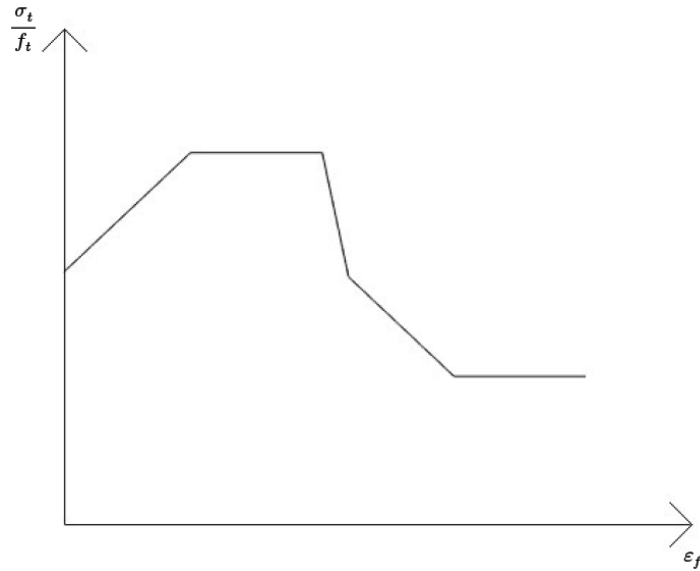
Figure 5.10: Tension function

5.3.1.2 Compressive Function

As it is known that SFRC concrete is more ductile than ordinary concrete, the first point in the default compressive function (fig. 5.11) is multiplied by 100 as recommended (Červenka et al.; 2016). The points defining the compressive function are given in table 5.3.
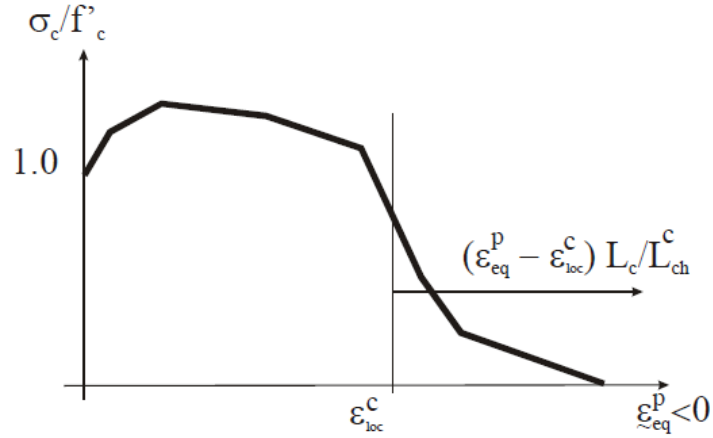
Figure 5.11: Compressive function (Červenka et al.; 2016)

	Point 1	Point 2	Point 3	Point 4
ε_{pl}	0.0	-4.206E-4	-8.411E-4	-5.841E-1
$\frac{\sigma_c}{f_c}$	0.25	0.8	1.0	0.0

Table 5.3: Points describing the compressive function for the FRC FEM-section

5.3.2 Reinforcement

The reinforcement's properties are automatically generated per the definitions in EN 1992 by GiD. All the reinforcement is defined as quality B500NC as per EN 1992, i.e. $\varepsilon_{ud} = 3.0\%$, and with the safety format set to characteristic (Figure 5.12) Input parameters are listed in table 5.4.

Material name		1D Reinforcement	
Material Prototype		CCReinforcement	
Reinforcement Function		Bilinear	
Young's Modulus	E_s	200	GPa
Characteristic Yield Strength	f_{yk}	500	MPa
Reinforcement Class		C	
Safety Format		Characteristic	
Hardening		Elastic - Perfectly Plastic	
Bond Slip		FIB MC 2010 (See section 2.6.5.1)	

Table 5.4: Input parameters for the reinforcement
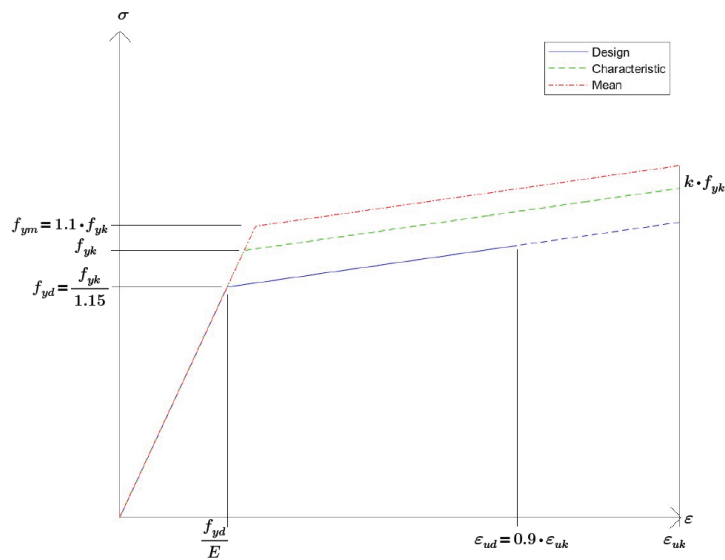
Figure 5.12: Safety formats for reinforcement (Červenka et al.; 2016)

5.3.3 Steel plates

As the loading applied isn't expected to cause the steel plates to undergo plastic deformations, a perfectly elastic material model is used, which simplifies the finite element calculations.

The steel plates are assigned the Solid elastic material model, with properties given in table 5.5.

Material type		Solid elastic	
Material Prototype		CC3DElastIsothropic	
Young's Modulus	E_s	200	GPa
Poisson's Ratio	ν	0.3	

Table 5.5: Input parameters for the steel plates

5.4 Analysis and Results

For each class, a FEM-analysis has been carried out, and in the following section the results from these FEM-analyses are compared to theoretical shear resistance, calculated using eqs. (4.1), (4.4) and (4.9) with all safety factors, i.e. γ_c, γ_s, and γ_{sf}, set equal to 1.0.
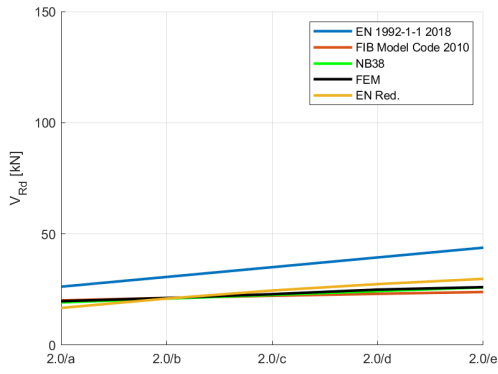
(a) Class 2.0
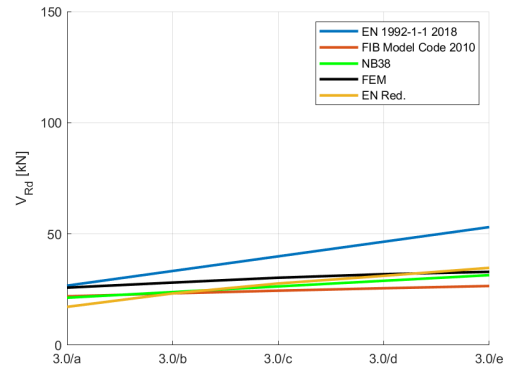
(b) Class 3.0
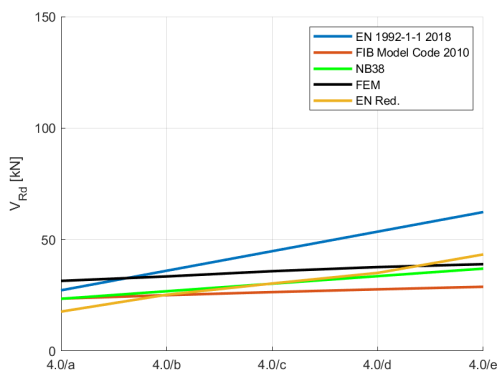
(c) Class 4.0
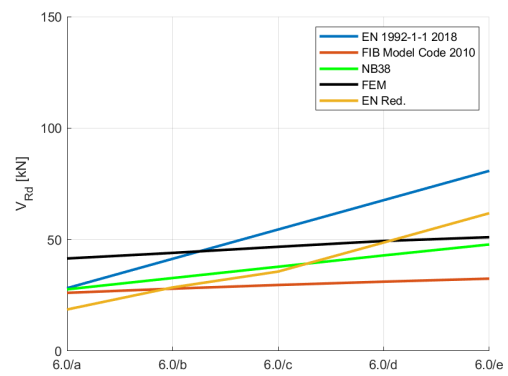
(d) Class 6.0
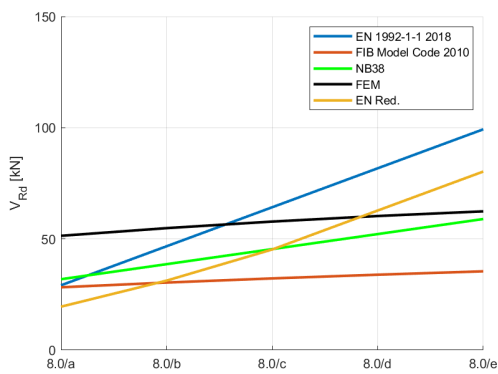
(e) Class 8.0
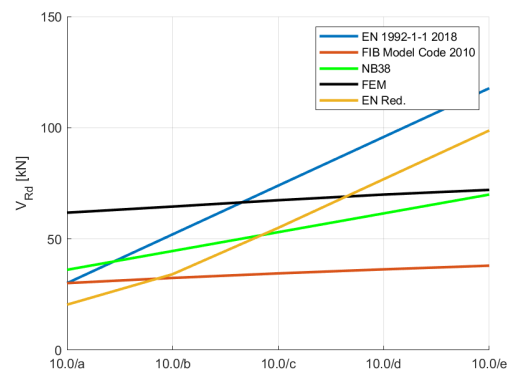
(f) Class 10.0

Figure 5.13: V_{Rd} of section shown in fig. 5.1 with increasing flexural strengths $f_{R,1k}$ and $f_{R,3k}$ compared to results from FEM-Analysis

As can be seen in fig. 5.13, for class 2.0 and 3.0 (figs. 5.13a and 5.13b) EN 1992-1-1:2018 overestimates the effect of the fibres regardless of $f_{R,3k}$, overestimating the shear capacity by 68% for class 2.0/e. Increasing $f_{R,1k}$, i.e. class 4.0 to 10.0 leads to the calculations from EN 1992-1-1:2018 to be conservative for class a, while significantly overestimating the capacity for class e, which indicate calculations that are too dependent on $\frac{f_{R,3k}}{f_{R,1k}}$. i.e. the FEM-analyses shows that the factor α_{t3} (eq. (4.1)) should be modified. For all classes - the calculations from FIB Model Code 2010 and NB38 are on the safe side. NB38 shows results gradually increasing towards the shear capacity from the FEM-analyses as $\frac{f_{R,3k}}{f_{R,1k}}$ increases, but with a significantly steeper gradient, i.e. a clear tendency to excessively favour an increase in $\frac{f_{R,3k}}{f_{R,1k}}$ with respect to the shear capacity is shown. The calculations from FIB Model Code 2010 shows a gradient approximately equal to the gradient of the FEM-results ($\Delta V_{Rd} = \chi \cdot \frac{f_{R,3k}}{f_{R,1k}}$, table 5.7), but with a lower dependency on $f_{R,1k}$, suggesting that the calculations for f_{ftu} is a bit on the safe side compared to FEM results.

The MAPE (Mean Average Percentage Error) of the different design guidelines vs. the FEM results are given in table 5.6.

	EN	FIB	NB38
Class 2.0	51.29%	4.25%	1.8%
Class 3.0	32.11%	18.15%	11.91%
Class 4.0	29.67%	25.85%	15.40%
Class 6.0	30.02%	36.73%	19.53%
Class 8.0	32.80%	44.17%	21.59%
Class 10.0	36.18%	49.03%	21.78%

Table 5.6: MAPE Comparison of calculations vs. FEM results

Class	EN	EN Red.	NB	FIB	FEM
2	21.9425	16.339	8.458	4.698	8.2175
3	32.9075	21.513	12.6875	5.7955	8.9975
4	43.87	30.548	16.9165	6.6445	9.6
6	65.7835	53.281	25.374	7.9455	12.225
8	87.685	76.5275	33.833	8.9495	13.725
10	109.5755	99.71	42.2915	9.7785	12.95

Table 5.7: χ - Slope of $V_{Rd}/\frac{f_{R,3k}}{f_{R,1k}}$

It is worth noticing that the slope - χ - for EN and NB is a constant function of $f_{R,1k}$, respectively $\approx 10.97 \cdot f_{R,1k}$ and $\approx 4.23 \cdot f_{R,1k}$, while for FIB and the FEM analysis, χ is approximately equal to $3.89 + 0.62 \cdot f_{R,1k}$ and $7.13 + 0.70 \cdot f_{R,1k}$ respectively. On the next page, a from eqs. (4.12) to (4.16), are compared. In addition to comparing a from the guidelines, a_{FEM} is calculated as follows:

$$a_{FEM} = \frac{\frac{V_{Rd,FEM}}{b_w d} - \frac{0.6}{\eta \gamma_c} \left(100 \cdot \rho_l \cdot f_{ck} \cdot \frac{d_{dg}}{d} \right)^{1/3}}{f_{ftuk,EN}} \tag{5.1}$$
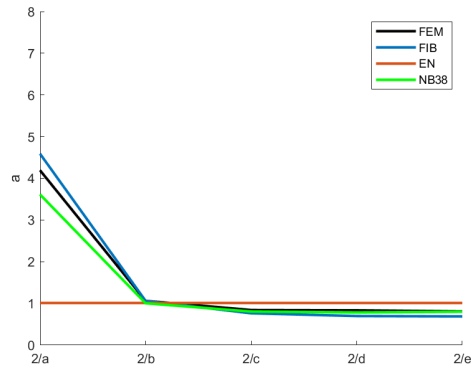
(a) Class 2.0
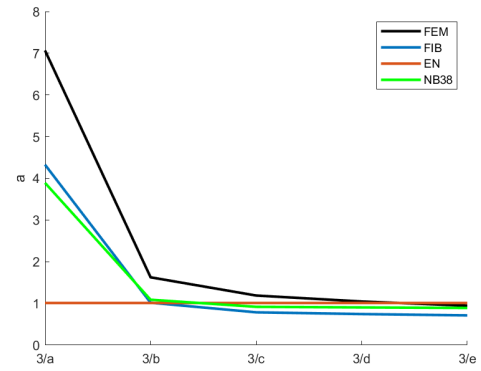
(b) Class 3.0
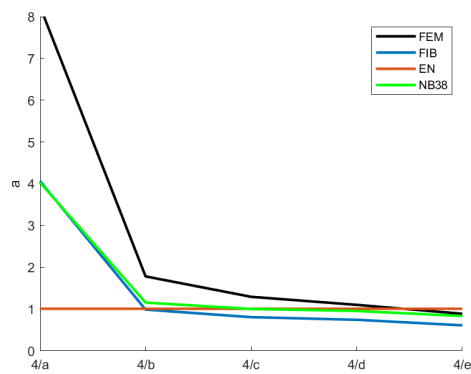
(c) Class 4.0
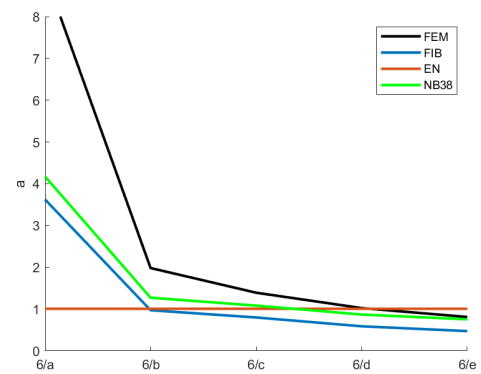
(d) Class 6.0
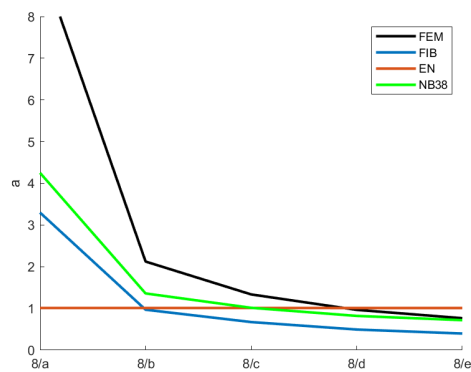
(e) Class 8.0
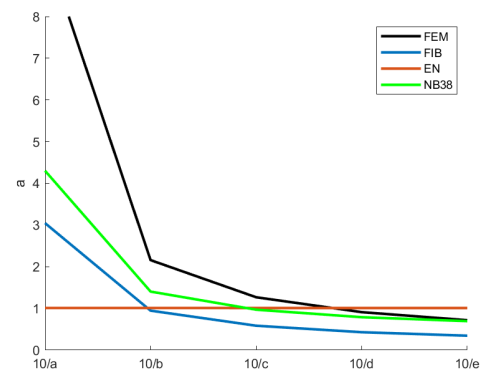
(f) Class 10.0

Figure 5.14: Comparison of variable a of section shown in fig. 5.1 with increasing flexural strengths $f_{R,1k}$ and $f_{R,3k}$ compared to a from FEM

Comparing the graphs in fig. 5.14, we can define Δa as the difference between $a_{guideline}$ and a_{fem} - i.e. $\Delta a = a_{guideline} - a_{fem}$. Δa is positive when the guideline overestimates the contribution of the fibres, and negative when not. i.e. negative values are conservative with respect to the behaviour seen in the FEM-analysis, and thus safe calculation wise.

Guideline	Class	a	b	c	d	e
EN	2.0	-3.1822	-0.0510	0.1693	0.1766	0.2031
	3.0	-6.0562	-0.6158	-0.1787	-0.0360	0.0653
	4.0	-7.2347	-0.7746	-0.2863	-0.0935	0.1193
	6.0	-8.0110	-0.9747	-0.3846	-0.0164	0.1958
	8.0	-8.3646	-1.1141	-0.3258	0.0442	0.2442
	10.0	-8.6866	-1.1486	-0.2581	0.0990	0.2916
FIB	2.0	0.3973	-0.0002	-0.0782	-0.1366	-0.1193
	3.0	-2.7395	-0.6096	-0.4029	-0.3018	-0.2318
	4.0	-4.1830	-0.7946	-0.4868	-0.3571	-0.2766
	6.0	-5.3952	-1.0096	-0.5926	-0.4350	-0.3382
	8.0	-6.0763	-1.1553	-0.6629	-0.4718	-0.3679
	10.0	-6.6507	-1.2119	-0.6827	-0.4810	-0.3719
NB38	2.0	-0.5790	-0.0585	-0.0356	-0.0502	-0.0063
	3.0	-3.1755	-0.5375	-0.2709	-0.1421	-0.0543
	4.0	-4.2139	-0.6273	-0.2910	-0.1458	-0.0544
	6.0	-4.8463	-0.7096	-0.3094	-0.1543	-0.0564
	8.0	-5.1232	-0.7649	-0.3212	-0.1452	-0.0471
	10.0	-5.3943	-0.7546	-0.2982	-0.1211	-0.0230

Table 5.8: Δa for the different guidelines and classes

It is noted that the a value still neglects v_{min} from eqs. (4.1), (4.4) and (4.9), and it is apparent that while FIB and NB38 have a values below the FEM results, EN 1992-1-1:2018 overestimates the contribution of the fibres for classes c-e depending on $f_{R,1k}$. As table 5.8 shows, FIB Model Code 2010 also overestimates the contribution of the fibres for class 2.0/a. While this is true, the low values of $f_{R,1k}$ and $f_{R,3k}$ makes $\Delta V_{Rd} = 0.38$kN

6 Conclusion and suggestions for further work

6.1 Discussion and conclusions

The results from the calculations shows that it is apparent that the differences between FIB Model Code 2010, NB38, and EN 1992-1-1:2018 when calculating crack-widths and shear resistance are vast. The difference in calculated shear resistance between the guidelines is at maximum as high as 115.1kN (Class 10.0/e, $V_{Rd,EN} - V_{Rd,FIB}$).

A difference in the crack-width calculations was also found - FIB Model Code 2010 and NB38 give conservative values compared to EN 1992-1-1:2018. The crack-width of the beam in fig. 3.2 class 1.5/a exceeds w_{lim} when using the calculations from EN 1992, but FIB MC2010 and NB38 gives results lower than w_{lim}.

It is shown in chapter 5 that EN 1992-1-1:2018 overestimates the contribution from the fibres to the shear resistance compared to FEM results for most classes. For class 10.0/e EN 1992-1-1:2018 overestimates the shear resistance by $\approx$ 46kN - almost 64% higher than the result gained from the FEM-analysis.

6.2 Suggestions for further work

Although a lot of work - it would be interesting to check the results experimentally. Especially the shear resistances from chapter 5, as the shear resistance calculated with EN 1992-1-1:2018 might dramatically overestimate the real shear resistance - and thus lead to structural failure. As all of the calculations are based on a B35 (C35/45) concrete - achieving a class 10.0/e concrete might be impossible practically, and it would be interesting to look at how the guidelines deviate from experimental results.

References

Barragan, B. (2002). *Failure and toughness of steel fiber reinforced concrete under tension and shear*, PhD thesis, Universitat Politécnica de Catalunya,.

Benzley, S., Perry, E., Merkley, K., Clark, B. and Sjaardema, G. (1995). A comparison of all hexagonal and all tetrahedral finite element meshes for elastic and elasto-plastic analysis, *Proceedings, 4th International Meshing Roundtable* **17**.

Bigaj, A. (1999). *Structural Dependence of Rotational Capacity of Plastic Hinges in RC Beams and Slabs*, PhD thesis, TU Delft.

Borst, R. d. (1986). Nonlinear analysis of frictional materials.

Døssland, Å. L. (2008). *Fibre Reinforcement in Load Carrying Concrete Structures*, PhD thesis, NTNU.

EN 1992-1-1:2018 (2018). *Standard*, Comité européen de normalisation.

Červenka, V. et al. (2016). *Atena Theory*, Červenka Consulting.

FIB Model Code (2010). *Standard*, The International Federation for Structural Concrete.

Hwang, J.-H. et al. (2013). Shear behavior models of steel fiber reinforced concrete beams modifying softened truss model approaches, *Materials* **6**(10): 4847–4867.

Kanstad, T. (2019). Re: Crack-width calculations from en 1992-1-1:2018, Email.

Kanstad, T. et al. (2011). Forslag til retningslinjer for dimensjonering, utførelse og kontroll av fiberarmerte betongkonstruksjoner, *Technical report*, COIN Project report 29.

Löfgren, I. (2005). *Fibre-Reinforced Concrete for Industrial Construction - a fracture mechanics approach to material testing and structural analysis*, PhD thesis, Chalmers University of Technology.

Micallef, K., Sagaseta, J., Fernández Ruiz, M. and Muttoni, A. (2014). Assessing punching shear failure in reinforced concrete flat slabs subjected to localised impact loading, *International Journal of Impact Engineering* **71**.

Naaman, A. (2003). Engineered steel fibers with optimal properties for reinforcement of cement composites, *Journal of Advanced Concrete Technology* **1**(3): 241–252.

NB38 (n.d.). *Standard*, Norsk Betongforening.

Nordbrøden, H. H. and Weydahl, S. H. (2012). *Testing of fibre reinforced concrete structures - shear capacity of beams with corbel-end*, Master's thesis, NTNU.

Plizzari, G. (2019). Eurocode meeting: Frc crack control.

Rosenbusch, J. (2003). *Zur Querkrafttragfähigkeit von Balken aus Stahlfaserverstärktem Stahlbeton*, PhD thesis, TU Braunschweig.

Thorenfeldt, E. (2003). Theoretical tensile strength after cracking, fibre orientation and average stress in fibres, *Workshop Proceedings from A Nordic Miniseminar: Design Rules for Steel Fibre Reinforced Concrete Structures* pp. 43–60.

A Shear capacity calculations

EN 1992-1-1 2018

$h := 400$ $b := 200$

$c_{nom} := 35$ $f_{ck} := 35$ $f_{yk} := 500$

$\varnothing_s := 20$ $D_{lower} := 16$

$\gamma_{sf} := 1.5$ $\gamma_s := 1.15$

$\gamma_c := 1.5$ $\alpha_{cc} := 0.85$

$f_{yd} := \dfrac{f_{yk}}{\gamma_s}$ $f_{cd} := \dfrac{\alpha_{cc} \cdot f_{ck}}{\gamma_c}$

$d := h - c_{nom} - \dfrac{\varnothing_s}{2} = 355$

$n := 2$ number of ø20 bars

$A_{sl} := n \cdot \pi \cdot \left(\dfrac{\varnothing_s}{2}\right)^2$

$f_{R.1k} := 4.0$

$f_{R.3k} := 1.3 \cdot f_{R.1k} = 5.2$
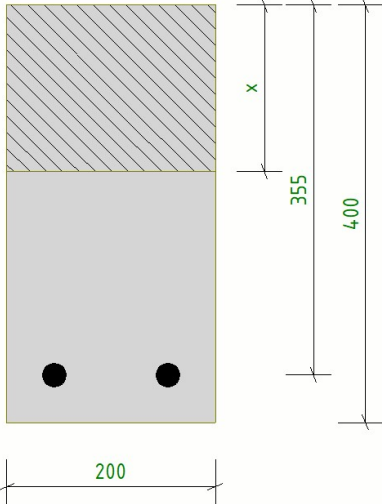
$f_{ftk.res.2.5} := 0.37 \cdot f_{R.3k}$

$f_{ftd.res.2.5} := \dfrac{f_{ftk.res.2.5}}{\gamma_{sf}}$

$x := \dfrac{A_{sl} \cdot f_{yd} + f_{ftd.res.2.5} \cdot b \cdot h}{0.8 \cdot f_{cd} \cdot b + f_{ftd.res.2.5} \cdot b}$
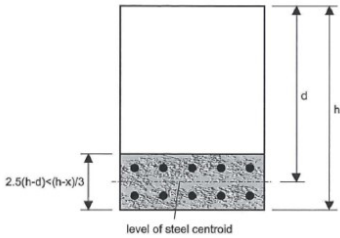
$A_{ct} := \left(min\left(2.5\ (h-d), \dfrac{(h-x)}{3}\right) \cdot b\right) \cdot mm^2 = 0.019\ m^2$

$\alpha_{t3} := 0.57 - 0.26\ \dfrac{f_{R.1k}}{f_{R.3k}}$

$f_{Ftuk} := \alpha_{t3} \cdot f_{R.3k} = 1.924$

$\kappa_O := 1.0$

$\kappa_G := min\left(1.0 + \left(\dfrac{A_{ct}}{m^2} \cdot 0.5\right), 1.5\right) = 1.01$

$f_{Ftu.ef} := \kappa_O \cdot \kappa_G \cdot f_{Ftuk}$

$f_{Ftud} := \dfrac{f_{Ftu.ef}}{\gamma_{sf}} = 1.295$

$$\eta := min\left(1 + 0.43 \cdot f_{Ftud}^{2.85}, 2.5\right) = 1.898$$

$$\rho_l := \frac{A_{sl}}{b \cdot d}$$

$$d_{dg} := min\left(16 + D_{lower}, 40\right)$$

$$\tau_{Rd.cf1} := \left(\frac{0.7}{\eta \cdot \gamma_c}\left(100 \cdot \rho_l \cdot f_{ck} \cdot \frac{d_{dg}}{d}\right)^{\frac{1}{3}} + f_{Ftud}\right) \cdot MPa = 1.641 \ MPa$$

$$\tau_{Rdc.min} := \left(\frac{10}{\gamma_c} \cdot \sqrt{\frac{f_{ck}}{f_{yd}} \cdot \frac{d_{dg}}{d}}\right) \cdot MPa = 0.568 \ MPa$$

$$\tau_{Rd.cf} := max\left(\tau_{Rd.cf1}, \tau_{Rdc.min} + f_{Ftud} \cdot MPa\right) = 1.863 \ MPa$$

$$V_{Rd} := \tau_{Rd.cf} \cdot b \cdot d \cdot mm^2 = 132.271 \ kN$$

b

Fib Model Code 2010

$h := 400$ $\qquad b := 200$

$c_{nom} := 35$ $\qquad f_{ck} := 35$ $\qquad f_{yk} := 500$
$\qquad\qquad\qquad f_{ctk} := 2.2$

$\varnothing_s := 20$ $\qquad D_{lower} := 16$

$\gamma_{sf} := 1.5$ $\qquad \gamma_s := 1.15$

$\gamma_c := 1.5$ $\qquad \alpha_{cc} := 0.85$

$f_{yd} := \dfrac{f_{yk}}{\gamma_s}$ $\qquad f_{cd} := \dfrac{\alpha_{cc} \cdot f_{ck}}{\gamma_c}$

$d := h - c_{nom} - \dfrac{\varnothing_s}{2} = 355$

$n := 2$ $\qquad\qquad\qquad\qquad\qquad f_{R.1k} := 4.0$

$A_{sl} := n \cdot \pi \cdot \left(\dfrac{\varnothing_s}{2}\right)^2$ $\qquad\qquad f_{R.3k} := 1.3 \cdot f_{R.1k} = 5.2$

$f_{Fts} := 0.45 \cdot f_{R.1k}$

$w_u := 1.5$

$CMOD_3 := 2.5$

$f_{Ftuk} := \max\left(f_{Fts} - \dfrac{w_u}{CMOD_3} \left(f_{Fts} - 0.5\, f_{R.3k} + 0.2\, f_{R.1k}\right), 0\right) = 1.8$

$k := min\left(1 + \sqrt{\dfrac{200}{d}}, 2\right)$

$\rho_l := \dfrac{A_{sl}}{b \cdot d}$

$\tau_{Rd.cf1} := \dfrac{0.18}{\gamma_c} \cdot k \cdot \left(100 \cdot \rho_l \cdot \left(1 + 7.5 \cdot \dfrac{f_{Ftuk}}{f_{ctk}}\right) \cdot f_{ck}\right)^{\frac{1}{3}} \cdot \boldsymbol{MPa} = 1.27 \ \boldsymbol{MPa}$

$\tau_{Rd.cf.min} := 0.035 \cdot k^{\frac{3}{2}} \cdot f_{ck}^{\frac{1}{2}} \cdot \boldsymbol{MPa} = 0.48 \ \boldsymbol{MPa}$
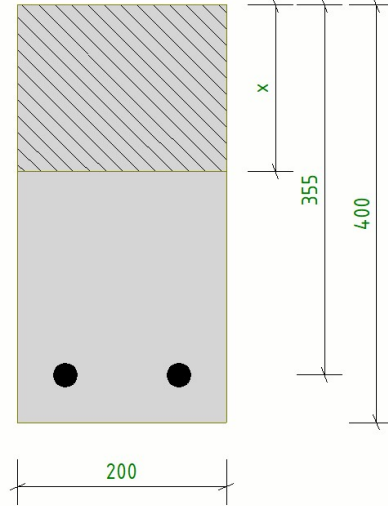
$$\tau_{Rd.cf} := \max\left(\tau_{Rd.cf1}, \tau_{Rd.cf.min}\right)$$

$$V_{Rd.f} := \tau_{Rd.cf} \cdot b \cdot d \cdot mm^2 = 90.18 \ kN$$

NB38

$h := 400$ $b := 200$

$c_{nom} := 35$ $f_{ck} := 35$ $f_{yk} := 500$
                       $f_{ctk} := 2.2$

$\varnothing_s := 20$ $D_{lower} := 16$

$\gamma_{sf} := 1.5$ $\gamma_s := 1.15$

$\gamma_c := 1.5$ $\alpha_{cc} := 0.85$

$f_{yd} := \dfrac{f_{yk}}{\gamma_s}$ $f_{cd} := \dfrac{\alpha_{cc} \cdot f_{ck}}{\gamma_c}$

$d := h - c_{nom} - \dfrac{\varnothing_s}{2} = 355$

$n := 2$ $f_{R.1k} := 4.0$

$A_{sl} := n \cdot \pi \cdot \left(\dfrac{\varnothing_s}{2}\right)^2$ $f_{R.3k} := 1.3 \cdot f_{R.1k} = 5.2$

$f_{ftk.res.2.5} := 0.37 \cdot f_{R.3k}$

$f_{ftd.res.2.5} := \dfrac{f_{ftk.res.2.5}}{\gamma_{sf}}$

$k_2 := 0.18$

$C_{Rd.c} := \dfrac{k_2}{\gamma_c}$

$k := min\left(1 + \sqrt{\dfrac{200}{d}} , 2\right)$

$\rho_l := \dfrac{A_{sl}}{b \cdot d}$

$\tau_{Rd.ct} := max\left(C_{Rd.c} \cdot k \cdot \left(100 \cdot \rho_l \cdot f_{ck}\right)^{\frac{1}{3}} , 0.035 \cdot k^{\frac{2}{3}} \cdot f_{ck}^{\frac{1}{2}}\right) \cdot \boldsymbol{MPa}$

$\tau_{Rd.cf} := 0.6 \cdot f_{ftd.res.2.5} \cdot \boldsymbol{MPa}$
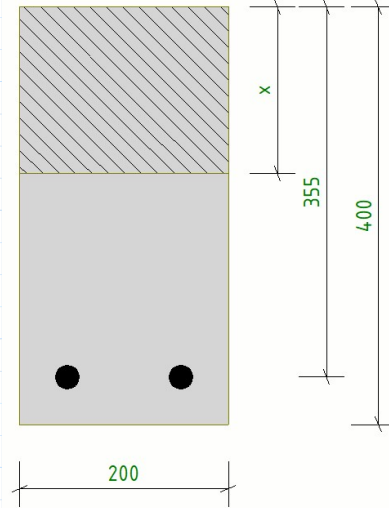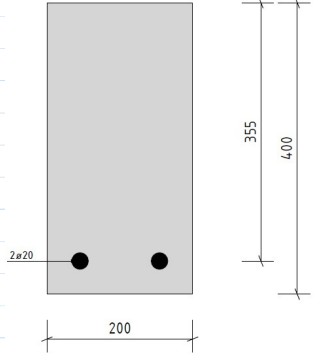
$$\tau_{Rd.c} := \tau_{Rd.ct} + \tau_{Rd.cf} = 1.429 \; \boldsymbol{MPa}$$

$$V_{Rd} := \tau_{Rd.c} \cdot b \cdot d \cdot \boldsymbol{mm}^2 = 101.482 \; \boldsymbol{kN}$$

B Crack Width calculations

EN 1992-1-1:2018

$h := 400 \; mm$ $\qquad b := 200 \; mm$

$c_{nom} := 35 \; mm$ $\qquad f_{ck} := 35 \; MPa \; f_{yk} := 500 \; MPa$

$\varnothing_l := 20 \; mm$ $\qquad f_{ctm} := 3.2 \; MPa$

$\gamma_{sf} := 1.0$ $\qquad D_{lower} := 16 \; mm$

$\gamma_c := 1.0$ $\qquad \gamma_s := 1.0$

$f_{R.1k} := 2.5 \; MPa$ $\qquad\qquad A_s := 2 \cdot \pi \cdot \left(\dfrac{\varnothing_l}{2}\right)^2 = 628.319 \; mm^2$

$f_{R.3k} := 0.5 \cdot f_{R.1k} = 1.25 \; MPa$ $\qquad\qquad d := h - c_{nom} - \dfrac{\varnothing_l}{2} = 0.355 \; m$

$k_b := 0.8$ $\qquad\qquad\qquad$ From matlab:

$\qquad\qquad\qquad\qquad\qquad\qquad \sigma_s := 381.763 \; MPa \qquad x := 98.1937 \; mm$

$A_{ct} := \left(min\left(2.5 \; (h-d), \dfrac{(h-x)}{3} \right) \cdot b \right) = 0.02 \; m^2$

$\rho_{p.ef} := \dfrac{2 \cdot \pi \cdot \left(\dfrac{\varnothing_l}{2}\right)^2}{A_{ct}}$

$\alpha_{t3} := 0.57 - 0.26 \cdot \dfrac{f_{R.1k}}{f_{R.3k}} = 0.05$

$\alpha_{t1} := 0.53 - 0.14 \cdot \dfrac{f_{R.3k}}{f_{R.1k}} = 0.46$

$\kappa_O := 1.0$

$\kappa_G := min\left(1.0 + 0.5 \cdot \dfrac{A_{ct}}{m^2}, 1.5 \right) = 1.01$

$f_{Fts.ef} := \kappa_O \cdot \kappa_G \cdot \alpha_{t1} \cdot f_{R.1k} = 1.162 \; MPa$

$S_{r.max.cal} := \left(2 \cdot c_{nom} + 0.35 \cdot k_b \cdot \dfrac{\varnothing_l}{\rho_{p.ef}} \right) \cdot \left(1 - \dfrac{f_{Fts.ef}}{f_{ctm}} \right) = 158.824 \; mm$

$\varepsilon_{sm} - \varepsilon_{cm} = \dfrac{\sigma_s - k_t \cdot \dfrac{f_{ctm}}{\rho_{p.ef}} \; (1 + \alpha_e \cdot \rho_{p.ef})}{E_s} \geq 0.6 \; \dfrac{\sigma_s}{E_s}$
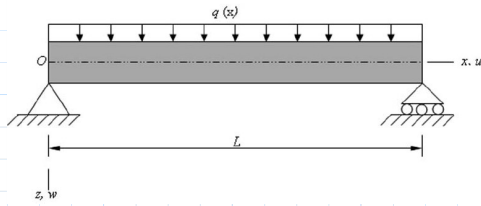
$$q := 25 \ \frac{kN}{m}$$

$$L := 5 \ m$$

$$M_{Ek} := \frac{q \cdot L^2}{8} = 78.125 \ kN \cdot m$$

$$f_{ftuk} := \alpha_{t3} \cdot f_{R.3k} = 0.062 \ MPa$$

$$f_{ftu.ef} := \kappa_O \cdot \kappa_G \cdot f_{ftuk} = 0.063 \ MPa$$

$$f_{ftud} := \frac{f_{ftu.ef}}{\gamma_{sf}} = 0.063 \ MPa$$

$$k_t := 0.6$$

$$E_s := 200 \ GPa$$

$$E_c := 34 \ GPa$$

$$\alpha_e := \frac{E_s}{E_c}$$

$$\varepsilon_{sm} - \varepsilon_{cm} = \varepsilon_{sm.cm}$$

$$\varepsilon_{sm.cm} := \max\left(\frac{\sigma_s - k_t \cdot \dfrac{f_{ctm}}{\rho_{p.ef}} \left(1 + \alpha_e \cdot \rho_{p.ef}\right)}{E_s}, \ 0.6 \cdot \frac{\sigma_s}{E_s}\right) = 0.002$$

$$w_{k.cal} := S_{r.max.cal} \cdot \varepsilon_{sm.cm} = 0.245 \ mm$$

h

Fib MC 2010 / NB38

$h := 400 \; mm \qquad b := 200 \; mm$

$c_{nom} := 35 \; mm \qquad f_{ck} := 35 \; MPa \qquad f_{yk} := 500 \; MPa$

$\varnothing_l := 20 \; mm \qquad f_{ctm} := 3.2 \; MPa$

$\gamma_{sf} := 1.0 \qquad D_{lower} := 16$

$\gamma_c := 1.0 \qquad \gamma_s := 1.0$

$f_{R.1k} := 2.5 \; MPa$

$f_{R.3k} := 0.7 \cdot f_{R.1k} = 1.75 \; MPa$

$d := h - c_{nom} - \dfrac{\varnothing_l}{2}$

$A_s := 2 \cdot \pi \cdot \left(\dfrac{\varnothing_l}{2}\right)^2$

$k := 1.0 \qquad\qquad A_c := b \cdot h$

$c := c_{nom} \qquad\qquad E_s := 200 \; GPa$

Short term, instantaneous loading: $\qquad E_c := 34 \; GPa$

$\tau_{bms} := 1.8 \cdot f_{ctm}$

$\beta := 0.6$

$\eta_r := 0$

From matlab:

$\sigma_s := 291.9024 \; MPa \qquad x := 115.2511 \; mm$

$A_{ct} := \left(min\left(2.5 \; (h-d), \dfrac{(h-x)}{3}\right) \cdot b\right) = 0.019 \; m^2$

$\rho_{s.ef} := \dfrac{A_s}{A_{ct}}$

$\alpha_e := \dfrac{E_s}{E_c}$

$f_{ftsk} := 0.45 \cdot f_{R.1k} = 1.125 \; MPa \qquad\qquad f_{ftsd} := \dfrac{f_{ftsk}}{\gamma_{sf}} = 1.125 \; MPa$

$f_{ftsm} := \dfrac{f_{ftsk}}{0.7} = 1.607 \; MPa$

i
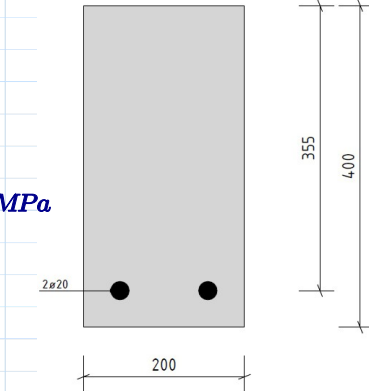
$$\sigma_{sr} := \frac{\left(f_{ctm} - f_{ftsm}\right) \cdot \left(1 + \alpha_e \cdot \rho_{s.ef}\right)}{\rho_{s.ef}}$$

$$S_{r.max} := 2 \left(k \cdot c + \frac{1}{4} \cdot \frac{\varnothing_l}{\rho_{s.ef}} \cdot \frac{\left(f_{ctm} - f_{ftsm}\right)}{\tau_{bms}}\right) = 153.55 \ \pmb{mm}$$

$$w_d := 2 \left(k \cdot c + \frac{1}{4} \cdot \frac{\varnothing_l}{\rho_{s.ef}} \cdot \frac{\left(f_{ctm} - f_{ftsm}\right)}{\tau_{bms}}\right) \cdot \frac{1}{E_s} \left(\sigma_s - \beta \cdot \sigma_{sr}\right) = 0.198 \ \pmb{mm}$$

j

C Iterative solution of steel stress in simply supported SFRC section subject to bending

```matlab
clear
clc

% Inputs:
q=10; % kN/m
L=5; % m
Ec=34*10^3; % MPa
Es=200*10^3; % MPa
h=400; % mm
b=200; % mm
d=355; % mm
As=628.319; % mm^2
fftk=0.888; %MPa, fftk,res,2.5


stop=0;
M=(q*L^2/8)*10^6;
x(1,1)=0.45*d;
eps0(1,1)=M/(0.5*Ec*b*x(1,1)*(h/2+x(1,1)/6)+Es*As*((d-x(1,1))/
x(1,1))*(d-x(1,1)/2-h/2));
epss(1,1)=(d-x(1,1))/(x(1,1))*eps0(1,1);
x(1,2)=(Es*epss(1,1)*As+fftk*b*h)/(0.5*Ec*eps0(1,1)*b+fftk*b);
ss(1,1)=Es*epss(1,1);
i=2;

while abs(x(1,i)-x(1,i-1))>0.000001 % Iterative calculation running
 until x converges.
    eps0(1,i)=M/(0.5*Ec*b*x(1,i)*(h/2+x(1,i)/6)+Es*As*((d-x(1,i))/
x(1,i))*(d-x(1,i)/2-h/2));
    epss(1,i)=(d-x(1,i))/(x(1,i))*eps0(1,i);
    if epss(1,i) > 500/Es % Checks if steel strain is above yield, and
 cancels if so
        disp(['Warning: steel strain is above yield'])
        stop=1;
        break
    end
    ss(1,i)=Es*epss(1,i);
    i=i+1;
    x(1,i)=(Es*epss(1,i-1)*As+fftk*b*h)/(0.5*Ec*eps0(1,i-1)*b+fftk*b);
end

if stop~=1
    disp(['x=', num2str(x(end)), ' mm, and steel stress = ',
 num2str(Es*epss(end)), ' MPa'])
    subplot(2,1,1)
    plot(x)
    title('Convergence of x')
    xlabel('Steps')
    ylabel('x [mm]')
    subplot(2,1,2)
    plot(ss)
    title('Convergence of \sigma_s')
```

```
    xlabel('Steps')
    ylabel('\sigma_s [MPa]')
end
```

x=122.823 mm, and steel stress = 103.3652 MPa

l
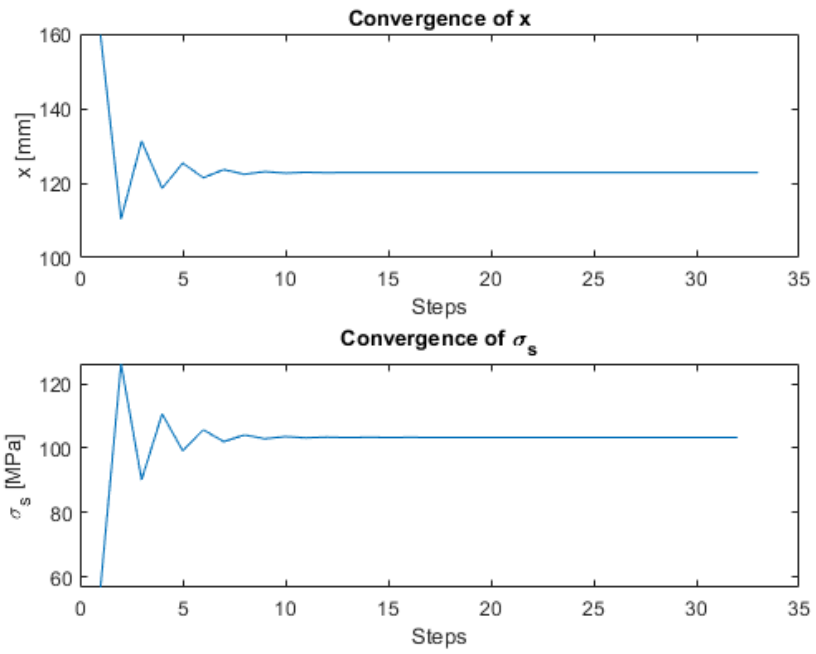
D   Calculation of the factor a_{FIB} according to eq. (4.13)

$$\tau := \frac{0.18}{\boxed{\gamma_c}} \cdot k \cdot \left(100 \cdot \rho_l \cdot \left(1 + 7.5 \cdot \frac{f_{ftuk.fib}}{f_{ctk}}\right) \cdot f_{ck}\right)^{\frac{1}{3}} = \frac{0.6}{\eta \cdot \gamma_c} \cdot \left(100 \cdot \rho_l \cdot f_{ck} \cdot \frac{d_{dg}}{d}\right)^{\frac{1}{3}} + a_{FIB} \cdot f_{ftuk.EN}$$

$$\tau \xrightarrow{solve, a_{FIB}} -\frac{0.02 \cdot \left(30.0 \cdot \left(\frac{100.0 \cdot d_{dg} \cdot f_{ck} \cdot \rho_l}{d}\right)^{\frac{1}{3}} - 9.0 \cdot \eta \cdot k \cdot \left(\frac{100.0 \cdot f_{ck} \cdot \rho_l \cdot f_{ctk} + 750.0 \cdot f_{ck} \cdot \rho_l \cdot f_{ftuk.fib}}{f_{ctk}}\right)^{\frac{1}{3}}\right)}{\eta \cdot \gamma_c \cdot f_{ftuk.EN}}$$

$d_{dg} := 32$	$\gamma_c := 1.5$	$f_{Fts} := 0.45 \cdot \boxed{f_{R.1k}}$	
$d := 355$		$w_u := 1.5$	$\kappa_O := 1.0$
$f_{ck} := 35$		$CMOD_3 := 2.5$	

$$\rho_l := \frac{2 \cdot \pi \cdot 3^2}{200 \cdot d} \qquad f_{ftuk.fib} := \boxed{f_{Fts}} - \frac{w_u}{CMOD_3}\left(f_{Fts} - 0.5\, f_{R.3k} + 0.2\, f_{R.1k}\right)$$

$$k := 1 + \sqrt{\frac{200}{d}} \qquad f_{ftuk.EN} := \left(0.57 - 0.26\, \boxed{\frac{f_{R.1k}}{f_{R.3k}}}\right) \cdot f_{R.3k}$$

$$f_{ctk} := 2.2$$

$$\eta = min\left(1 + 0.43 \cdot \left(\frac{\kappa_O \cdot \kappa_G}{\gamma_{sf}} \cdot f_{ftuk.EN}\right)^{2.85}, 2.5\right)$$

$$\tau := \frac{0.18}{\gamma_c} \cdot k \cdot \left(100 \cdot \rho_l \cdot \left(1 + 7.5 \cdot \boxed{\frac{f_{ftuk.fib}}{f_{ctk}}}\right) \cdot f_{ck}\right)^{\frac{1}{3}} = \frac{0.6}{\eta \cdot \gamma_c} \cdot \left(100 \cdot \rho_l \cdot f_{ck} \cdot \frac{d_{dg}}{d}\right)^{\frac{1}{3}} + a_{FIB} \cdot f_{ftuk.EN}$$

$$a_{FIB} := \tau \xrightarrow{solve, a_{FIB}, float, 5} -\frac{1.0 \cdot \left(5.2518 \cdot 10^6 \cdot \eta \cdot \left(0.57019 \cdot f_{R.1k} + 2.851 \cdot f_{R.3k} + 2.7876\right)^{\frac{1}{3}} - 6.3103 \cdot 10^6\right)}{6.5 \cdot 10^6 \cdot \eta \cdot f_{R.1k} - 1.425 \cdot 10^7 \cdot \eta \cdot f_{R.3k}}$$

$$a_{FIB} \xrightarrow{simplify} -\frac{52518.0 \cdot \eta \cdot \left(0.57019 \cdot f_{R.1k} + 2.851 \cdot f_{R.3k} + 2.7876\right)^{\frac{1}{3}} - 63103.0}{\eta \cdot \left(65000.0 \cdot f_{R.1k} - 142500.0 \cdot f_{R.3k}\right)}$$

E Calculation of the factor a_{NB} according to eq. (4.16)

$$\tau := C_{Rd.c} \cdot k \cdot \left(100 \cdot \rho_l \cdot f_{ck}\right)^{\frac{1}{3}} + 0.6 \cdot f_{ftd.res.2.5} = \frac{0.6}{\eta \cdot \gamma_c} \cdot \left(100 \cdot \rho_l \cdot f_{ck} \cdot \frac{d_{dg}}{d}\right)^{\frac{1}{3}} + a_{NB} \cdot f_{ftuk.EN}$$

$$\tau \xrightarrow{solve,\, a_{NB}} \frac{0.6 \cdot f_{ftd.res.2.5} + C_{Rd.c} \cdot k \cdot \left(100 \cdot f_{ck} \cdot \rho_l\right)^{\frac{1}{3}} - \dfrac{0.6 \cdot \left(\dfrac{100 \cdot d_{dg} \cdot f_{ck} \cdot \rho_l}{d}\right)^{\frac{1}{3}}}{\eta \cdot \gamma_c}}{f_{ftuk.EN}}$$

$$\gamma_c := 1.5 \qquad \gamma_s := 1.15 \qquad \gamma_{sf} := 1.5 \qquad\qquad\qquad f_{ck} := 35$$

$$C_{Rd.c} := \frac{0.18}{\gamma_c} \qquad\qquad h := 400 \qquad\qquad c_{nom} := 35 \qquad\qquad \varnothing_l := 20 \qquad\qquad b := 200$$

$$d := h - c_{nom} - \frac{\varnothing_l}{2} \qquad\qquad A_{sl} := 2 \cdot \pi \cdot \left(\frac{\varnothing_l}{2}\right)^2 \qquad\qquad d_{dg} := 32$$

$$k := 1 + \sqrt{\frac{200}{d}}$$

$$\rho_l := \frac{A_{sl}}{b \cdot d}$$

$$\kappa_O := 1.0$$

$$f_{ftk.res.2.5} := 0.37 \cdot f_{R.3k}$$

$$f_{ftd.res.2.5} := \frac{f_{ftk.res.2.5}}{\gamma_{sf}} \qquad\qquad\qquad \kappa_G := min\left(1.0 + A_{ct} \cdot 0.5, 1.5\right)$$

$$f_{ftuk.EN} := \left(0.57 - 0.26 \frac{f_{R.1k}}{f_{R.3k}}\right) \cdot f_{R.3k}$$

$$\eta = min\left(1 + 0.43 \cdot \left(\frac{\kappa_O \cdot \kappa_G}{\gamma_{sf}} \cdot f_{ftuk.EN}\right)^{2.85}, 2.5\right)$$

$$\tau := C_{Rd.c} \cdot k \cdot \left(100 \cdot \rho_l \cdot f_{ck}\right)^{\frac{1}{3}} + 0.6 \cdot f_{ftd.res.2.5} = \frac{0.6}{\eta \cdot \gamma_c} \cdot \left(100 \cdot \rho_l \cdot f_{ck} \cdot \frac{d_{dg}}{d}\right)^{\frac{1}{3}} + a_{NB} \cdot f_{ftuk.EN}$$

$$a_{NB} := \tau \xrightarrow{solve,\, a_{NB},\, float,\, 5} -\frac{1.0 \cdot \left(1.6493 \cdot 10^7 \cdot \eta + 3.7 \cdot 10^6 \cdot \eta \cdot f_{R.3k} - 1.4081 \cdot 10^7\right)}{6.5 \cdot 10^6 \cdot \eta \cdot f_{R.1k} - 1.425 \cdot 10^7 \cdot \eta \cdot f_{R.3k}}$$

$$a_{NB} \xrightarrow{simplify} -\frac{16493.0 \cdot \eta + 3700.0 \cdot \eta \cdot f_{R.3k} - 14081.0}{\eta \cdot \left(6500.0 \cdot f_{R.1k} - 14250.0 \cdot f_{R.3k}\right)}$$

n

F V_{Rd} results from EN, FIB, and NB38 for section shown in fig. 4.3

B35, 2ø20, h=400, b=200, ULS				
Class	EN	EN Red	FIB	NB38
2.0/a	42.76	42.429	62.989	57.348
2.0/b	53.883	53.4	66.339	61.552
2.0/c	65.003	63.843	69.382	65.755
2.0/d	76.118	73.486	72.179	69.958
2.0/e	87.229	82.237	74.774	74.161
3.0/a	43.979	43.646	68.647	62.602
3.0/b	60.659	59.847	72.845	68.907
3.0/c	77.329	74.482	76.609	75.212
3.0/d	93.991	87.171	80.035	81.517
3.0/e	110.644	98.517	83.191	87.822
4.0/a	45.198	44.859	73.5	67.856
4.0/b	67.43	66.023	78.359	76.263
4.0/c	89.646	84.031	82.681	84.669
4.0/d	111.847	99.314	86.593	93.076
4.0/e	134.035	114.238	90.18	101.482
6.0/a	47.633	47.277	81.643	78.364
6.0/b	80.96	77.406	87.518	90.974
6.0/c	114.253	100.906	92.694	103.584
6.0/d	147.516	123.919	97.35	116.193
6.0/e	180.749	156.425	101.598	128.803
8.0/a	50.067	49.677	88.423	88.872
8.0/b	94.475	87.515	95.079	105.65
8.0/c	138.828	117.611	100.914	122.498
8.0/d	183.129	158.804	106.143	139.311
8.0/e	227.381	203.057	110.902	156.124
10.0/a	52.498	52.056	94.298	99.38
10.0/b	107.976	96.745	101.598	120.396
10.0/c	163.372	139.047	107.977	141.412
10.0/d	218.691	194.366	113.68	162.428
10.0/e	273.939	249.615	118.863	183.444

G V_{Rd} results from EN, FIB, NB38, and FEM-analyses for section shown in fig. 5.2

B35, 2⌀6, h=150, b=150, SLS					
Class	EN	EN Red	FIB	NB38	FEM
2.0/a	26.262	16.714	20.124	19.194	19.745
2.0/b	30.652	20.925	21.194	20.885	21.195
2.0/c	35.04	24.552	22.166	22.577	22.92
2.0/d	39.429	27.439	23.06	24.269	24.97
2.0/e	43.816	29.796	23.889	25.96	26.075
3.0/a	26.744	17.192	21.931	21.308	25.845
3.0/b	33.327	23.223	23.273	23.846	28.115
3.0/c	39.909	27.717	24.475	26.383	30.3
3.0/d	46.49	31.145	25.57	28.921	31.9
3.0/e	53.07	34.744	26.578	31.458	32.95
4.0/a	27.225	17.668	23.482	23.423	31.45
4.0/b	36.001	25.246	25.034	26.806	33.45
4.0/c	44.776	30.281	26.415	30.189	35.8
4.0/d	53.549	35.034	27.665	33.573	37.65
4.0/e	62.321	43.322	28.811	36.956	38.95
6.0/a	28.187	18.609	26.083	27.652	41.5
6.0/b	41.349	28.514	27.96	32.727	44
6.0/c	54.508	35.628	29.614	37.802	46.75
6.0/d	67.662	48.664	31.101	42.877	49.35
6.0/e	80.814	61.815	32.458	47.951	51.05
8.0/a	29.149	19.531	28.249	31.881	51.4
8.0/b	46.695	31.249	30.376	38.647	54.85
8.0/c	64.235	45.237	32.24	45.414	57.8
8.0/d	81.769	62.77	33.911	52.181	60.3
8.0/e	99.297	80.298	35.431	58.947	62.4
10.0/a	30.11	20.43	30.126	36.11	61.8
10.0/b	52.04	34.135	32.458	44.568	64.55
10.0/c	73.959	54.96	34.496	53.026	67.4
10.0/d	95.869	76.871	36.319	61.485	69.95
10.0/e	117.771	98.772	37.974	69.943	72.05

p